Lifetime Imaging Techniques for Optical Microscopy

Wolfgang Becker, Axel Bergmann
Becker & Hickl GmbH, Berlin, becker@becker-hickl.com, bergmann@becker-hickl.com

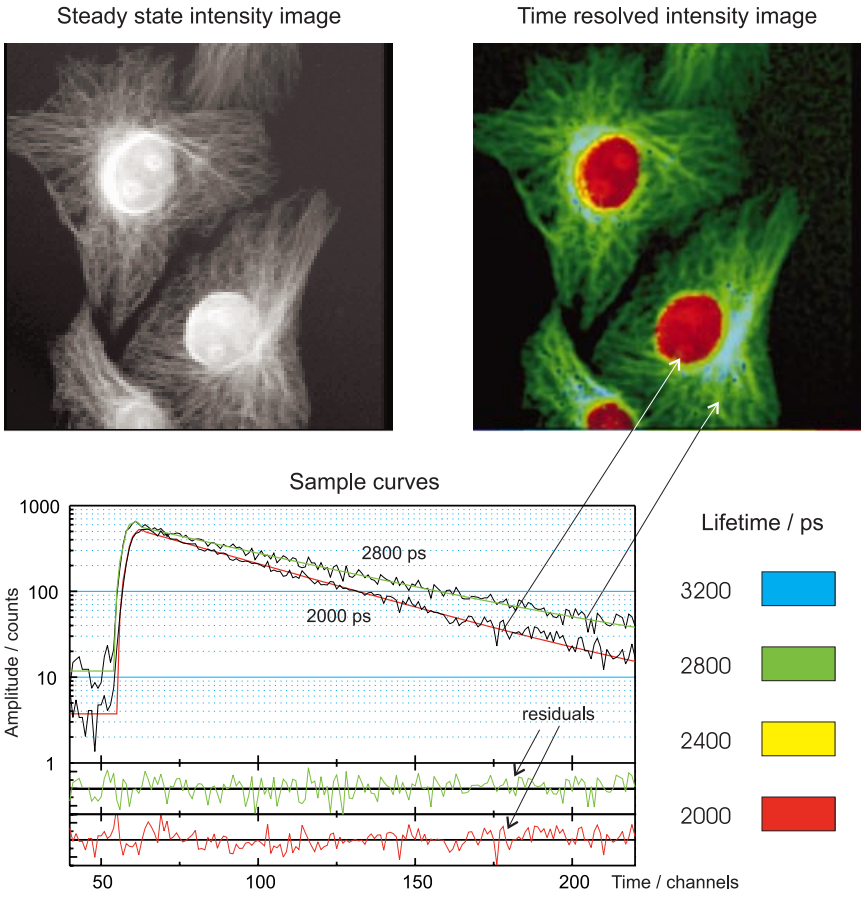

Contents

Introduction

Since their broad introduction in the early 90s confocal and two-photon laser scanning microscopes have initiated a breakthrough in biomedical imaging [1-5]. The applicability of multi-photon excitation, the optical sectioning capability and the superior contrast of these instruments make them an ideal choice for fluorescence imaging of biological samples.

However, the fluorescence of organic molecules is not only characterised by the emission spectrum, it has also a characteristic lifetime. Any energy transfer between an excited molecule and its environment in a predictable way changes the fluorescence lifetime. Since the lifetime does not depend on the concentration of the chromophore fluorescence lifetime imaging is a direct approach to all effects that involve energy transfer [6-10]. Typical examples are the mapping of cell parameters such as pH, ion concentrations or oxygen saturation by fluorescence quenching, or fluorescence resonance energy transfer (FRET) [6,7,8] between different chromophores in the cell. Furthermore, combined intensity / lifetime imaging is a powerful tool to distinguish between different fluorescence markers in multi-stained samples and between different natural fluorophores of the cells themselves. These components often have ill-defined fluorescence spectra but are clearly distinguished by their fluorescence lifetime [70].

Fluorescence lifetime measurements require a pulsed or modulated excitation source, a sufficiently fast detector and a suitable recording electronics. This article gives an overview about applicable time-resolved signal recording techniques and their benefits and drawbacks.

Biological Applications of Lifetime Techniques

When a dye molecule absorbs a photon it goes into an excited state from which it can return by the emission of a fluorescence photon, by converting the absorbed energy internally, or by transferring the energy to the environment (fig. 1) [6,9,10]. The probability that one of these effects occurs is independent of the time after the excitation. If a large number of similar molecules with similar local environment is excited by a short laser pulse the fluorescence decay function is therefore single exponential. As long as no energy is transferred to the environment the lifetime is the 'natural fluorescence lifetime', τ_0 which is a constant for a given molecule and refraction index of the solvent. The fluorescence decay times of the fluorophores commonly used in microscopy are of the order of a few ns.

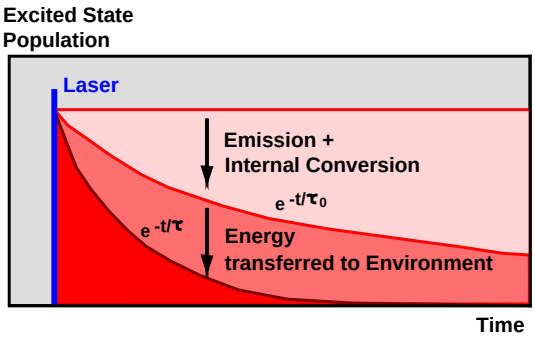

Fig. 1: Return of molecules from the excited state

Fluorescence Quenching

If energy is transferred to the environment the actual fluorescence lifetime, τ, is less than the natural lifetime, τ_0. For almost all dyes the energy transfer rate depends more or less on the concentration of ions, on the oxygen concentration, on the pH value or on the binding to proteins in a cell [6,9,10]. Therefore, specifically designed dyes can be used to probe the concentration of biological relevant ions such as Na^+, Mg^{++}, or Ca^{++}, the oxygen concentration or the pH value inside a cell. There is a direct relation between the lifetime and the quencher

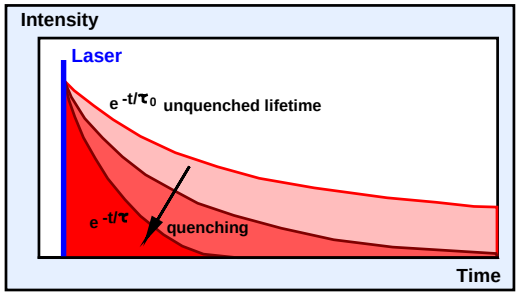

Fig. 2: Fluorescence quenching

concentration, fig. 2.

Fluorescence markers used to reveal particular protein structures in cells often bind to a variety of slightly different targets. Although this often does not cause significant changes in their spectral behaviour the lifetime can be clearly different due to different quenching efficiency. Therefore the lifetime of markers can be used as an additional probe technique in cells [11, 12]. A wide variety of chromophores including CFP, GFP and YFP clearly show variations in their fluorescence lifetimes. Although most of these effects are not investigated in detail yet there is probably a large potential for 'intelligent' markers based on lifetime changes.

Fluorescence can be almost entirely quenched in aggregates of fluorophore molecules. Lifetimes as short as 20 ps have been found. The fast relaxation is often considered unfavourable for photodynamic therapy applications. However, if the aggregates monomerise inside a tumor cell the effect can be of particular interest [52].

Resonance Energy Transfer

A particularly efficient energy transfer process is fluorescence resonance energy transfer, or FRET. FRET occurs if two different dyes are present with the emission band of one dye overlapping the absorption band of the other [6,7,8]. In this case the energy from the first dye, the donor, goes immediately into the second one, the acceptor. This results in an extremely efficient quenching of the donor fluorescence and, consequently, decrease of the donor lifetime, see fig. 3.

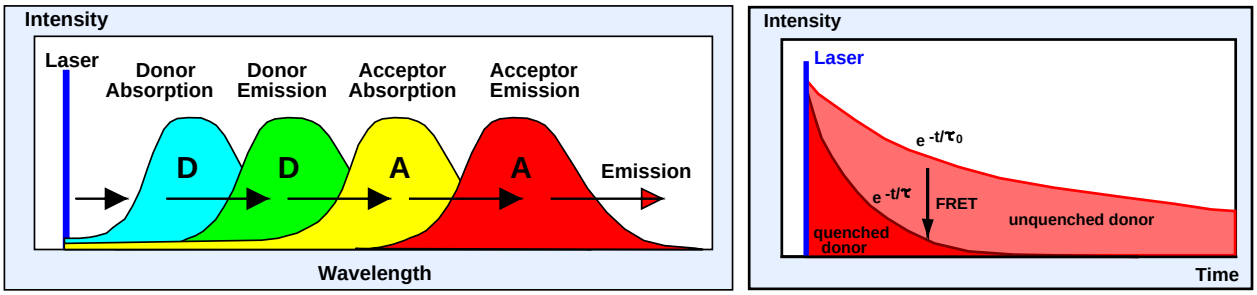

Fig. 3: Fluorescence Resonance Energy Transfer (FRET)

FRET works only over a distance shorter than a few nm. Therefore, it can be used to probe the distance between different subunits in the cell.

It is difficult to obtain quantitative FRET results from steady-state images. The fluorescence intensity does not only depend on the FRET efficiency but also on the unknown concentration of the dyes. Moreover, some of the acceptor molecules are excited directly, and the donor emission band extends into the acceptor emission. Up to eight measurements at different excitation wavelength and in different emission wavelength bands are required to obtain calibrated FRET results from steady state data [4,5,7]. FRET results can also be obtained by measuring the donor fluorescence, then photobleaching the acceptor, and measuring the donor once more. The FRET efficiency is given by the ratio of the two donor images. Although this procedure looks reliable at first glance photobleaching products may induce damage in the cell, and in a living cell diffusion may replace a part of the photobleached acceptor molecules.

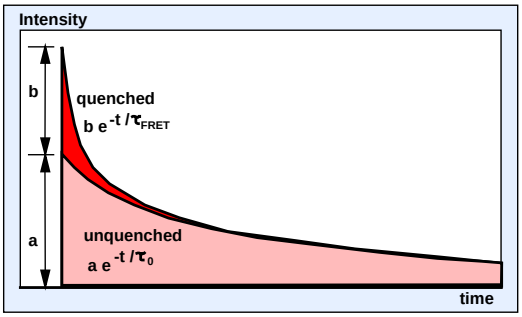

Fig. 4: Fluorescence decay components in FRET systems

In lifetime data, however, FRET shows up as a dramatical decrease of the donor lifetime [6,8,68,72]. The fluorescence decay functions contain the fluorescence of quenched and of unquenched donor

molecules and are therefore double-exponential, fig. 4. Qualitative FRET results can be obtained from the lifetime of a single exponential approximation of the decay curve. Quantitative measurements require double exponential decay analysis that delivers the lifetimes, τ_0 and $\tau_{FRET,}$ and the intensity factors, a and b, of the two decay components [68,72]. The relative numbers of quenched and unquenched molecules is given by the ratio of the two intensity components, b/a, while the average coupling efficiency of the FRET pairs is given by τ_0 / τ_{FRET}. In principle, both the ratio of quenched and unquenched molecules and the coupling efficiency can be derived from a single donor lifetime measurement.

Separation of Different Chromophores

Steady-state multi-wavelength techniques have been developed that efficiently separate different fluorescence markers by unmixing their fluorescence spectra [13]. However, not all marker combinations can efficiently be resolved. Even the well known GFP and YFP are difficult to unmix. Autofluorescence images of cells and tissue show a wide variety of fluorescence components with ill-defined, variable, and often unknown spectra. When spectral unmixing fails the components can usually be distinguished by their different lifetimes [70,75]. The relative concentration of two components can be determined by double-exponential decay analysis. Even if only a single exponential approximation, i.e. an average lifetime is measured, the contrast in the fluorescence images can be considerably improved. [70,75]. Moreover, changes in the relative concentration and the lifetime of autofluorescence components can possibly be used as diagnostic tools.

Significant progress can be expected from combining spectral unmixing and lifetime analysis. Recording of time- and wavelength resolved data is technically possible by TCSPC techniques (see ‘Multi Wavelength TCSPC Imaging’). Combining the two methods requires to develop suitable data analysis software.

Diffusion in Cells

Diffusion time constants in cells are usually in the ms range and below. They are usually determined by fluorescence correlation (FCS) techniques [14,15,16]. The problem is that the correlation technique is a single point measurement. Moreover, the measurement is usually not done in the same setup as the cell imaging. This makes it difficult to identify the measured spot in a particular cell with sufficient accuracy. Basically the photon counting techniques used for lifetime measurement are able to run a combined FCS and lifetime measurement at a single, well defined point of the sample. This could not only help to solve the positioning problem but also to identify single marker molecules [17] and to reveal conformational changes of the diffusing marker/protein clusters [18]. Although appropriate photon counters are available [63] no combined FLIM / FCS setup has become known yet.

Microscopy Techniques

Wide-Field Fluorescence Microscopy

As in any traditional microscope, the sample is uniformly illuminated by the excitation light. The image is detected by a CCD camera (fig. 5). To obtain time resolution in a wide-field setup the excitation light is pulsed or modulated and a gain modulated or gated intensified CCD camera is used [19,20,21,23]. The restriction to a special detection technique with sub-optimal efficiency is a drawback of wide-field imaging. Furthermore, wide-field imaging does not have the inherent depth resolution of the scanning techniques (see section below). However, there is a remarkable technique to obtain 3D images in whole-field microscopes [22], and a time-resolved solution with a gated CCD camera is described in [23]. The most severe drawback of the wide-field technique is that it cannot be used for two-photon excitation - a technique that allows deep tissue imaging in scanning microscopes.

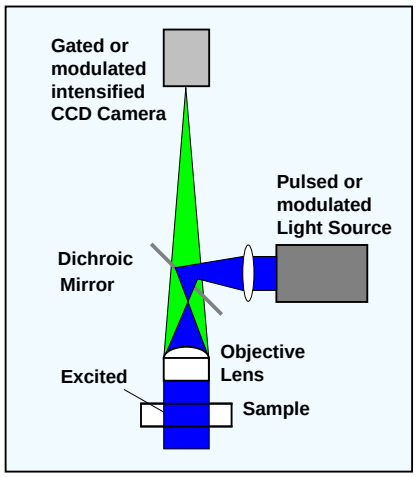

Fig. 5: Whole-field fluorescence lifetime imaging

A benefit of wide-field imaging is that it probably causes less photobleaching than the scanning techniques. Provided the same number of detected photons and the same detection efficiency, the overall excitation dose for wide-field imaging is the same as for the scanning techniques described below. However, the excitation density is much smaller because the light is not focused. Since the increase of photobleaching with the power is nonlinear it should be expected that wide field imaging is less affected by photobleaching than scanning techniques. Wide field techniques are therefore superior for time-lapse imaging, i.e. for recording sequences of images in millisecond intervals. For fluorescence lifetime imaging the situation may be less favourable because the detection techniques applicable for wide-field imaging are not the most efficient ones [39].

Laser Scanning Microscopy

The general optical principle of a laser scanning microscope [1,2] is shown in fig. 6.

The laser is fed into the optical path via a dichroic mirror and focused into the sample by the microscope objective lens. In the traditional confocal setup used for one-photon excitation (fig. 6, left) the light from the sample goes back through the objective lens, through the scanner, is diverted by a dichroic mirror and goes through a pinhole in the upper image plane of the objective lens. Light from outside the focal plane is not focused into the pinhole and therefore substantially suppressed. X-Y imaging is achieved by optically scanning the laser spot over the sample, Z imaging (optical sectioning) is possible by moving the sample or the microscope up and down.

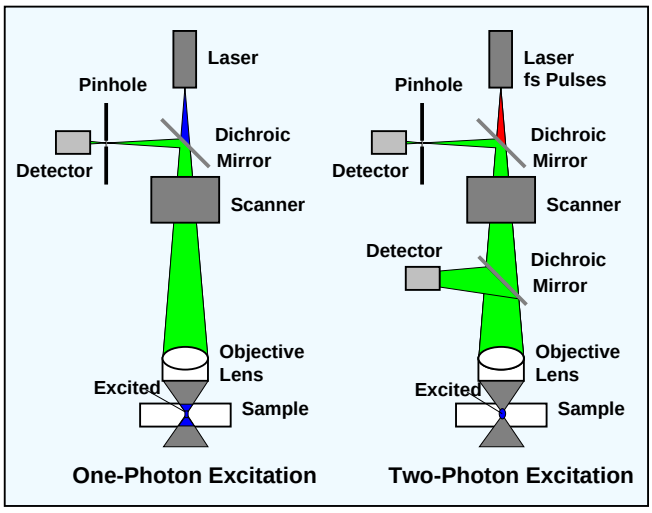

Fig. 6: General setup of a laser scanning microscope

With a fs Ti:Sa laser the sample can be excited by two-photon absorption [3,54,78]. Excitation occurs only in the focus, so that no pinhole is required to reject light from outside the focal plane.

Therefore, the fluorescence light need not be fed back through the scanner and through the pinhole. It can be diverted by a dichroic mirror directly behind the microscope objective. This setup is called ‘non-descanned detection’ in contrast to the ‘descanned detection’ shown above.

Two-photon excitation in conjunction with non-descanned detection can be used to image tissue layers as deep as 500 µm. Since the scattering and the absorption at the wavelength of the two-photon excitation are small the laser beam penetrates through relatively thick tissue. Even if there is some loss on the way through the tissue it can easily compensated by increasing the laser power. The increased power does not cause much photodamage because the power density outside the focus is small. However, as long as there are enough ballistic (non-scattered) excitation photons in the focus the fluorescence is excited. Of course, the fluorescence photons are heavily scattered on their way out of the tissue and therefore emerge from a relatively large area of the sample surface which is out of the focus of the objective. However, for non-descanned detection there is no need to focus the fluorescence light anywhere. Therefore the fluorescence photons can be efficiently transferred to the detector.

It is sometimes believed that lifetime imaging is somehow connected to two-photon excitation. This is, of course, not correct. Depending on the signal processing technique used, lifetime imaging requires a pulsed or modulated laser. Although a Ti:Sa laser is the ideal source lifetime imaging is possible with the frequency doubled Ti:Sa laser, with pulsed diode lasers, or with modulated CW lasers.

Optical Near-Field Microscopy

The optical near-field microscope (SNOM or NSOM) combines the principles of the atomic force microscope and the laser scanning microscope [24-28]. A sharp tip is scanned over the sample and kept in a distance comparable to the diameter of a single molecule. The tip can be the end of a tapered fibre through which the laser is fed to the sample (fig. 7, left). Or, the tip is illuminated by focusing the laser through the microscope objective on it and the evanescent field at the tip is used to probe the sample structure (fig. 7, right). In any case, the fluorescence photons are collected through the microscope objective.

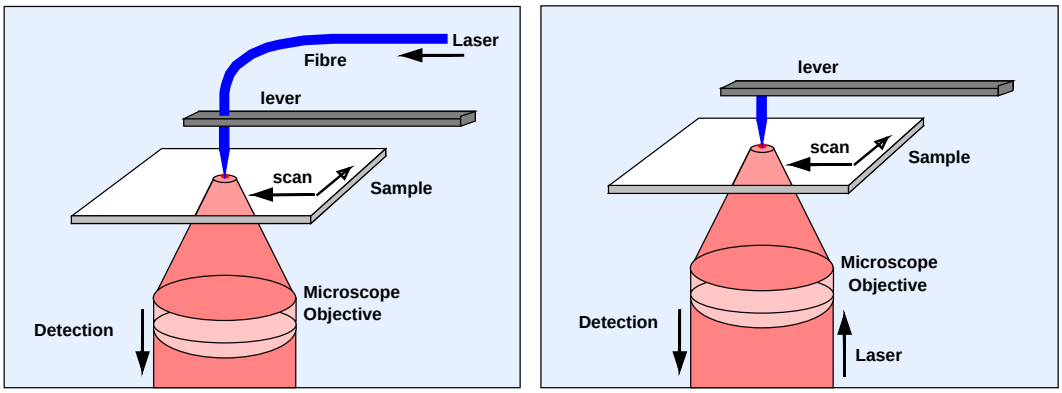

Fig. 7: Optical near-field microscope

The optical near-field microscope reaches a resolution of a few 10 nm, i.e. about 10 times less than the laser scanning microscope. Imaging cells with this technique is difficult and possibly restricted to special cases [27,28]. The realm of the optical near-field microscope are certainly applications where fluorescing molecules or nano-particles are fixed on a flat substrate.

Generally, the SNOM principle can be combined with flourescence lifetime imaging in the same way as the normal laser scanning microscope. Since only a small number of photons can be obtained from the extremely small sample volume photon counting techniquesare used to obtain lifetime information [78]. The problem to be expected is that the proximity of the tip changes the

fluorescence lifetime of the sample. Whether this effect makes lifetime imaging in a SNOM useless or whether it can be exploited for completely new techniques is hard to say.

Light Sources

Depending on the signal processing technique used, fluorescence lifetime imaging requires either a pulsed excitation source with a repetition rate in the MHz range or a modulated light source with a possible variable modulation frequency of 50 MHz to 1 GHz and a near perfect modulation depth.

Titanium-Sapphire Lasers

The ultimate solution is the femtosecond Ti:Sa laser. These lasers deliver pulses with 70 to 80 MHz repetition rate, 80 to 200 fs pulse width and up to several Watts average power. The wavelength is in the NIR from 780 nm to 950 nm. To excite the sample which usually absorbs below 500 nm, simultaneous two photon excitation is used. Due to the short pulse width and the high energy density in the focus of the microscope the two-photon process works very efficiently. Therefore the traditional frequency doubling of the Ti:Sa radiation is not often used for laser scanning microscopes.

Frequency Doubled Titanium-Sapphire Lasers

Frequency doubled titanium-sapphire lasers can be used to excite the sample via the traditional one-photon absorption. Frequency doubling is achieved by a nonlinear crystal. The output power is in the mW range. Less than 50µW are required to excite a typical sample so that the available power is by far sufficient. Whether one-photon or two-photon excitation gives less photobleaching is still under discussion. In a some cases considerably higher count rates and less photodamage for one-photon excitation were reported [72].

Fibre Lasers

Another useful excitation source are fibre lasers. Fibre lasers are available for a wavelength of 780 nm and deliver pulses as short as 100 to 180 fs [29]. The average power is 10 to 20 mW. This is less than for the Ti:Sa laser but still sufficient for two-photon excitation. As a rule of thumb, the maximum useful power for biological samples and fs NIR excitation is 5 to 10 mW. A higher power kills the cells or cooks the sample. The benefit of the fibre laser is the small size, the high reliability and a lower price compared to the Ti:Sa laser. The drawback of the fibre laser is that it is not tuneable.

Pulsed Diode Lasers

A reasonable cost solution for one-photon excitation are pulsed diode lasers which are available for the NUV, blue, red, and near-infrared range [30-32]. These lasers deliver pulses with 40 to 400 ps duration and up to 80 MHz repetition rate. The average power is up to a few mW. However, the pulse width increases with the power. For pulses shorter than 100 ps the average power is of the order of a few 100 µW. Fig. 8 shows the typical pulse shape of a 405 nm picosecond diode laser.

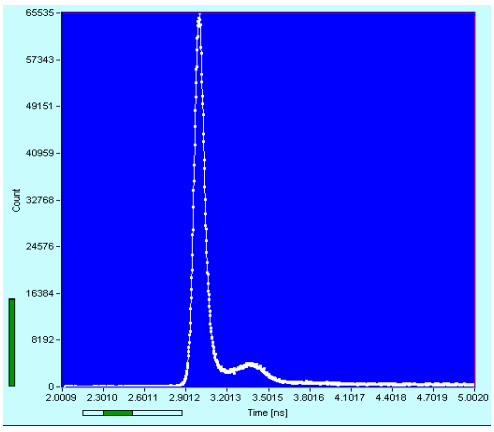

Fig. 8: Pulse shape of a blue diode laser. BDL-405, recorded with R3809U MCP and SPC-830 TCSPC module. FWHM is 80 ps.

Pulsing diodes with less than 100ps width requires special driving techniques that are not commonly available. However, pulses as narrow as 300 ps from red diodes can easily be obtained by connecting a commercially available pulse generator to a bare laser diode.

It has been shown that diode lasers can be used for time-resolved microscopy with good results [33, 33a]. Unfortunately the beam quality of diode lasers is not very good. Therefore it can be difficult to obtain a diffraction-limited resolution. However, if only the central part of the beam is used, the result can be quite acceptable. Discarding a large fraction of the beam causes a considerable loss of power. This loss is, however, not substantial because 50 µW in the focal plane are sufficient to excite the sample.

Modulated CW Lasers

For signal processing techniques based on phase measurement of modulated signals CW Ar+ and HeNe lasers in conjunction with an acousto-optical modulator can be used. However, care must be taken to avoid any crosstalk of the modulation frequency into the detection system. The smallest amount of crosstalk makes an accurate phase measurement impossible.

Using modulated CW lasers in conjunction with photon counting techniques is not recommended. These techniques require pulses rather than sinewave signals. Acousto-optical modulators are resonance systems unable to deliver sufficiently short pulses with high on/off ratio.

Mode-locked CW Lasers

Ar+ lasers can be actively mode-locked. By introducing a modulator into the laser cavity pulses as short as 100 ps with 80 to 120 MHz repetition rate are obtained. The pulses can be used directly or to pump a jet-stream dye laser that delivers ps pulses at a wavelength tuneable from 500 to 600 nm . Although the light from these lasers can be used for fluorescence excitation [65] the systems are often unstable and require permanent maintenance, checking and re-adjustment. We strongly discourage to use these lasers as excitation sources for time-resolved microscopy.

Pulse Pickers and Cavity Dumpers

Pulse pickers and cavity dumpers are used to obtain a lower repetition rate from lasers running at a high, fixed repetition rate. For fluorescence measurements they are sometimes used to measure lifetimes longer than the original period of the laser. The problem of the devices is the poor on-off ratio and the electrical noise they often produce. It is by far better to take some incomplete decay into regard in the data analysis than to cope with electrical noise and satellite pulses. Furthermore, a low repetition rate reduces the useful count rate in photon counting setups and possibly increases photobleaching. Don’t use pulse pickers if they are not absolutely necessary.

Detectors

Photomultiplier Tubes (PMTs)

The most common detectors for low level detection of light are photomultiplier tubes. A conventional photomultiplier tube (PMT) is a vacuum device which contains a photocathode, a number of dynodes (amplifying stages) and an anode which delivers the output signal (fig. 9).

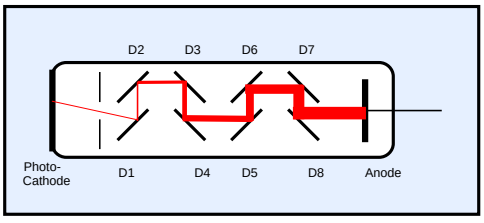

Fig. 9 Principle of a conventional PMT

The operating voltage builds up an electrical field that accelerates the electrons from the photocathode to the first dynode D1, from D1 to D2, further to the next dynodes, and from D8 to the anode. When a photoelectron emitted from the photocathode hits D1 it releases several secondary electrons. The same happens for the electrons emitted by D1 when they hit D2. The overall gain reaches values of 10^6 to 10^8. The secondary emission at the dynodes is very fast, therefore the secondary electrons resulting from one photoelectron arrive at the anode within a few

ns or less. Due to the high gain and the short response a single photoelectron yields a easily detectable current pulse at the anode.

A similar gain effect is achieved in the channel plate of a microchannel PMT, fig. 10. The channel plate consists of millions of narrow parallel channels. The channels have a diameter below 10 µm and are coated with a conductive material. When a high voltage is applied across the plate the walls of the channels act as secondary emission targets. With two plates in series, a gain of the order of 10^6 is achieved. MCP PMTs deliver extremely fast pulses with low transit time jitter.

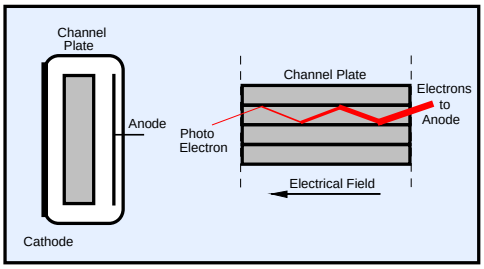

Fig. 10 Multichannel PMT

There are two parameters that characterise the time resolution of a photomultiplier - the 'Single Electron Response', SER, and the 'Transit Time Spread', TTS.

The SER is the output pulse for the detection of a single photon. The width of the SER limits the resolution of a PMT when it is used as a linear detector, i.e. a oscilloscope of fast digitizer. Some typical SER shapes for PMTs are shown in fig. 11.

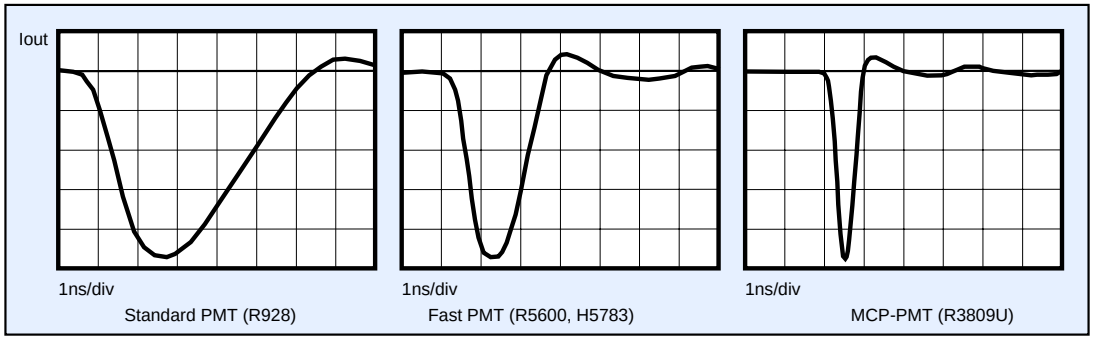

Fig. 11: Single Electron Response (SER) for typical PMTs

For photon counting applications the resolution is not limited by the width of the single electron response. For these techniques only the Transit Time Spread (TTS), i.e. the uncertainty of the delay between the photon detection and the output pulse is important. The TTS can be 10 times smaller than the width of the SER - a serious argument to use photon counting techniques in conjunction with photomultipliers.

Due to the random nature of the detector gain, the pulse amplitude is not stable but varies from pulse to pulse. The pulse height distribution can be very broad, up to 1:5 to 1:10. Fig. 12 (right) shows the SER pulses of an R5600 PMT. The pulse height jitter introduces an additional noise factor into all measurements that use the PMT as a linear detector. The signal-to-noise ratio of photon counting measurements is not - or almost not - impaired by the pulse height jitter.

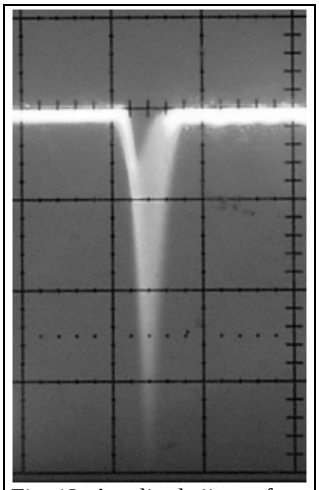

Fig. 12: Amplitude jitter of SER pulses (R5600)

If a PMT is operated near its full gain the peak current of the SER pulses is of the order of a few mA. This is much more than the allowed continuous output current. Consequently, for high repetition rate signals or steady state operation the PMT delivers a train of random pulses rather than a continuous signal. Because each pulse represents the detection of an individual photon the pulse density - not the pulse amplitude - is a measure for the light intensity at the cathode of the PMT. Obviously, the pulse

density is measured best by counting the PMT pulses within subsequent time intervals. Therefore, the application of photon counting techniques is the logical consequence of the high gain and the high speed of photomultipliers.

The efficiency, i.e. the probability that a particular photon causes a pulse at the output of the PMT, depends on the efficiency of the photocathode. Unfortunately the sensitivity S of a photocathode is usually not given in units of quantum efficiency but in mA of photocurrent per Watt incident power. The quantum efficiency QE is

$$QE = S \frac{h\,c}{e\,\lambda} = \frac{S}{\lambda} \cdot 1.24 \cdot 10^{6} \frac{W\,m}{A}$$

The efficiency for the commonly used photocathodes is shown in fig. 13 (right). The QE of the conventional bialkali and multialkali cathodes reaches 20 to 25 % between 400 and 500 nm. The recently developed GaAsP cathode reaches 45 %. The GaAs cathode has an improved red sensitivity and is a good replacement for the multialkali above 600 nm.

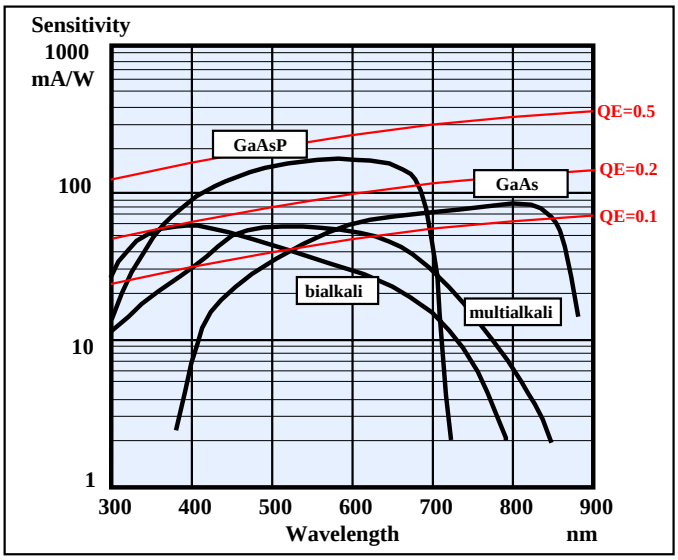

Fig. 13: Sensitivity of different photocathodes [34]

Generally, there is no significant difference between the efficiency of similar photocathodes in different PMTs and from different manufacturers. The differences are of the same order as the variation between different tube of the same type. Reflection type cathodes are a bit more efficient than transmission type photocathodes. However, reflection type photocathodes have non-uniform photoelectron transit times to the dynode system and therefore cannot be used in ultra-fast PMTs. A good overview about the characteristics of PMTs is given in [34] and [79].

Image intensifiers

Image intensifiers are vacuum devices consisting of a photocathode, an acceleration and/or multiplication system for the photoelectrons, and a two-dimensional image detection system.

First generation systems used a electron-optical imaging system that accelerates the photoelectrons to an energy of some keV and sends them to a fluorescent screen. The image from the screen was detected by a traditional camera or later with a CCD camera. First generation devices had a relatively low gain and strong image distortions.

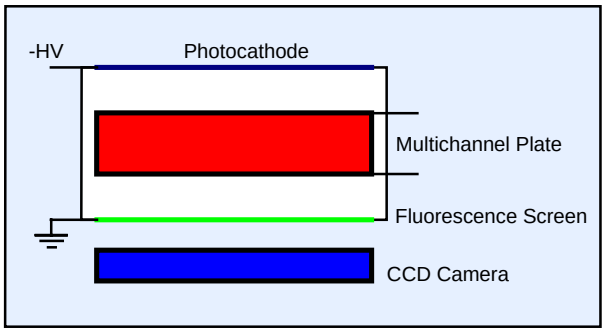

Fig. 14: Intensified CCD camera

Second generation image intensifiers use multichannel plates for electron multiplication (fig. 14). One plate gives a typical multiplication factor of 1000 so that a gain of 10^6 can be achieved by two plates in series.

The CCD chip can be placed inside the tube to detect the electrons directly. These EBD CCDs (Electron Bombarded CCDs) give higher gain than a CCD behind a fluorescent screen.

Gating of an image intensifier can be accomplished by a grid behind the photocathode. Gain modulation can also be achieved by modulating the voltage between the cathode and the channel plate or the voltage across the multichannel plate.

In general, image intensifiers use the same photocathodes as photomultiplier tubes. Therefore, the detection efficiency is approximately the same. There can, however, be an appreciable loss of photons or signal-to-noise ratio due to gating or modulating.

Avalanche photodiodes

Avalanche photodiodes (APDs) use a multiplication effect due to a strong electric field in a semiconductor structure (fig. 15). For use as a linear detector, a gain factor of the order of 100 can be achieved. However, cooled avalanche photodiodes can be used to detect single photons if they are operated close to or slightly above the breakdown voltage. The generated electron-hole pairs initiate an avalanche breakdown in the diode. Active or passive quenching circuits must be used to restore normal operation after each photon [36]. Therefore, a single photon avalanche photodiode (SPAPD) can only be used for photon counting. The advantage of an APD is the high quantum efficiency that can reach 90% in the near infrared. Single photon avalanche photodiode (SPAPD) modules are available from Perkin Elmer [35]. Although a resolution as fast as 20 ps has been reported for especially manufactured SPAPDs [36] the time resolution of these modules is in the order of 300 to 800 ps and depends on the count rate. This makes them less useful for lifetime measurements. SPAPDs are, however, excellently suited for fluorescence correlation measurements which do not require sub-ns resolution.

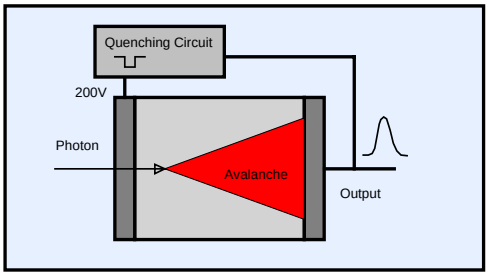

Fig. 15: Single Photon Avalanche Photodiode (SPAPD)

Cornerstones of Fluorescence Lifetime Imaging

Time Resolution

The lifetimes of highly efficient fluorescence markers are typically in the region of a few ns. However, these dyes are selected for high quantum yield. Lifetimes of less efficient chromophores can easily be below 100 ps. Quenching effects can reduce the lifetime down to a few 10 ps, and the lifetime of the quenched donor fluorescence in FRET experiments is in the order of 100 to 300 ps. Therefore, a good lifetime system should resolve fluorescence decay functions down to the order of 10 ps.

The fluorescence decay curves of in biological samples are often multi-exponential. There can be several chromophores in the same part of a cell, a single chromophore can be quenched witch non-uniform efficiency, or there can be quenched and unquenched molecules in the same part of the cell. Therefore, the ability to resolve multi-exponential decay functions is an absolute requirement to get quantitative results. Resolving two or even more exponential terms in a decay function requires data with an excellent signal-to-noise ratio.

Signal-to-Noise Ratio

Due to the short lifetimes, the measurement of fluorescence decay functions requires a detection bandwidth in the GHz range. The high bandwidth does not only demand for very fast detectors and detection electronics, it poses also a noise problem. The noise in fast optical measurements is almost essentially shot noise, i.e. the fluctuation of the number of photons detected within the resolving time of the measurement system. The best signal-to-noise ratio, SNR, that can be achieved is

$$SNR = n^{1/2}$$

with n being the number of photons detected within the resolved time interval. Actually the SNR can be even lower due to background signals originating in the detector or coming from the environment, random gain fluctuations in the detector, and inefficient acquisition of the detected photons in the subsequent signal processing chain.

Acceptable steady state images can be obtained for less than 100 photons detected per pixel of the image. However, lifetime measurements actually deliver a stack of images for - in case of time-domain methods - different times after the excitation or - in case of frequency domain methods - for different phases and modulation frequencies. Therefore, the number of photons required to get lifetime information is much larger. Although rough lifetime information for single exponential can be obtained from only 100 detected photons high accuracy measurements for multi-exponential decay analysis can easily require 10.000 or 100.000 photons per pixel [80].

Unfortunately the number of photons that can be emitted from the sample in a given time interval is limited by the sample itself.

Detection efficiency

The detection efficiency for the photons emitted be the sample depends on the optical system and on the detector. The efficiency of a microscope depends on the numerical aperture of the microscope objective, NA, and increases with NA^2. The effective NA can be doubled by using the 4Pi technique [37].

It is often claimed that the efficiency for non-descanned detection is considerably higher than for descanned detection. This is certainly true for deep-tissue imaging when the emission light is scattered in the sample and cannot be fed through a pinhole. However, state-of the art microscopes have pinholes with adjustable diameter. For imaging single cells there is no noticeable difference between descanned and non-descanned detection.

Appreciable loss of photons can occur in the filters used to select the desired emission wavelength range. Using the right filter for a particular chromophore can improve the efficiency considerably.

Commonly used detectors for lifetime imaging are described below. Although there is no appreciable difference between detectors of the same cathode type not all cathodes may be available for a particular detector. Techniques that are not restricted to a special detector, i.e. the photon counting techniques, can use high efficiency detectors, i.e. PMTs with GaAs cathodes or single photon avalanche photodiodes.

Recording efficiency

Different signal processing techniques differ considerably in terms of recording efficiency, i.e. in the exploitation of the detected photons. Taking into regard that the available number of photons is limited by photobleaching in the sample, the recording efficiency is the most important parameter next to the time resolution. The quality of a signal recording technique can be described by a 'figure of merit' [38, 39], F , that describes the ratio of the signal-to-noise ratio SNR of an ideal measurement to the signal-to-noise ration actually achieved, i.e.

$$F = \frac{SNR_{ideal}}{SNR_{act}}$$

F values for different methods were determined in [39]. Since the SNR is proportional to the square root of the number of detected photons, n, the efficiency of a technique in terms of photons required to obtain a given SNR is

$$E = 1 / F^2$$

The figure of merit and the efficiency will be used in the discussion of the commonly used lifetime techniques.

Sample Saturation

The sample volume from which the photons are detected in a laser scanning microscope is of the order of 1 fl. For a chromophore concentration of 10-6 mol/l this volume contains only 600 molecules, and for 10-9 mol/l the number of molecules is of the order of 1. Lifetime measurements require a pulsed or modulated light source. To avoid saturation effects for pulsed excitation only a small fraction of the molecules can be excited by each pulse. Therefore, lasers with repetition rates in the kHz range cannot reasonably be used in conjunction with scanning. There is, however, no saturation problem if lasers with a repetition rate above 50 MHz such as Ti:Sa lasers, YLF lasers or pulsed laser diodes are used.

Photobleaching

The most severe limit for the emission intensity is set by photobleaching in the sample. The chromophores are not infinitely stable but are destroyed after a large number of absorption and emission cycles. The reasons of photobleaching are not clear in detail and are probably different for one-photon and two-photon excitation . Possible reasons are simultaneous multi-photon absorption, intersystem crossing, reactions from the triplet state and excited-state absorption [40-45].

It is often claimed that photodamage and photobleaching is smaller for two-photon excitation. Certainly, there is no absorption outside the focus and consequently above and below the focal plane. Moreover, a cell can withstand much more power in the NIR than in the NUV because the fraction of absorbed power is much smaller [46,47]. However, if the cell contains dyes with a strong absorption around 400 nm and photobleaching is compared for the same number of emitted

fluorescence photons the situation is less clear. It has also been found that photobleaching is more rapid for two-photon excitation [41,42].

For two-photon excitation the dependence of the photobleaching efficiency on the excitation power is highly nonlinear. For photobleaching versus excitation power exponents of 2.5 [45] and from 3 to 5 for have been found [43]. At the same time the emission followed the excitation intensity by the expected power of 2. That means photobleaching increases more than linearly with the emission intensity. Therefore two-photon excitation can easily cause 10 times faster photobleaching than one-photon excitation for the same emission intensity [43].

Although photobleaching is the most crucial constraint for scanning microscopy the question about the excitation method is still open. The consequence from the controversial situation is not to rely on two-photon excitation alone. For all lasers commonly used for two-photon excitation frequency doubling is available and delivers sufficient power for one-photon excitation.

Signal Processing Techniques

Gated Image Intensifiers

Gating an image intensifier is achieved by placing a grid behind the photocathode. The principle is similar as for the grid in a radio tube. As long as the grid voltage is negative referred to the photocathode the photoelectrons cannot pass the grid. When a positive pulse is applied the electrons pass through the meshes of the grid and are accelerated towards the multichannel plate or into the acceleration system.

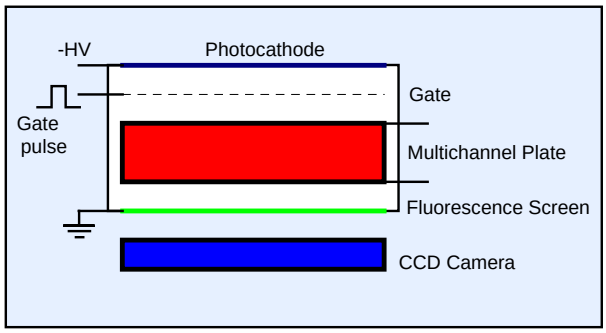

Fig. 16: Gated Image Intensifier

Although gating of an image intensifier looks straightforward at fist glance it is anything but simple, particularly if sub-ns resolution is to be achieved. Even if a sufficiently short gating pulse can be generated electronically the electrical field between the photocathode and the grid must follow the pulse at the same speed. Because the conductivity of the photocathode is relatively low the time constant formed by the gate-cathode capacitance and the cathode resistance limits the switching speed. Furthermore, a variable lateral field builds up in front of the photocathode that distorts the image and impairs the image resolution. Manufacturers counteract these effects by using high conductivity photocathodes which, however, compromises sensitivity. High efficiency GaAs and GaAsP photocathodes as they are used in PMTs have particularly low conductivity and are most likely not applicable for gated image intensifiers.

Another RC time constant exists between the grid and the multichannel plate. Although the change of the field in front of the plate has only small influence on the gating performance it induces a lateral current in the multichannel plate that heats the device at high gate repetition rates.

The gating resolution can also be impaired be electron-optical effects. When the gate voltage in the setup of fig. 16 is negative a cloud of photoelectrons builds up between the cathode and the grid. When a gate pulse is applied to the grid these electrons pass the grid and enter the detection system. Depending on the grid geometry, the lifetime of the photoelectrons between the grid and the cathode can be of the order of some 100 ps.

The effects described above can be reduced by additional grids. Even then a lateral change of the gate delay due to the wave propagation in the grid structure remains. This effect is, however, predictable and can be corrected in the recorded data.

Standard gated image intensifier devices have a minimum gate width of the order of a few ns. A device with 5ns gate width has been used to determine single exponential decay constants down to a few ns by deconvolution [33]. The shortest gate width obtained with gated image intensifiers is 50 ps for low repetition rate applications and 200 ps at a repetition rate of 80 MHz [20,51].

The general setup of a wide field and a scanning microscope with a gated image intensifier is shown in fig. 17.

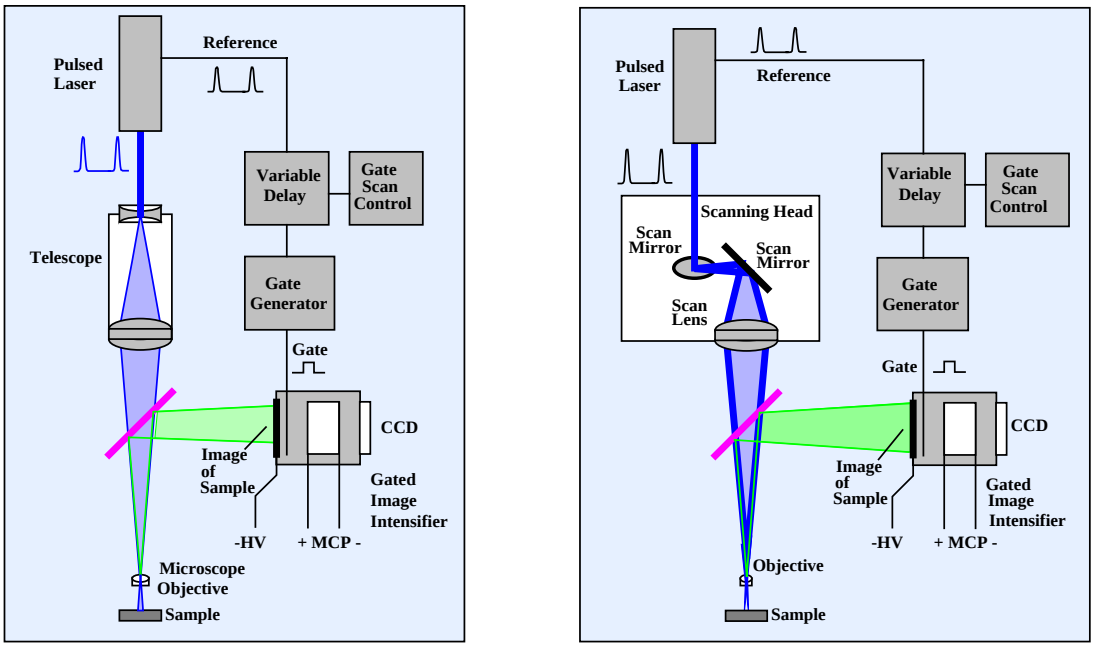

Fig. 17: Wide field microscope (left) and scanning microscope (right) with gated image intensifier

For time-resolved imaging a series of images is recorded for different delays of the gate pulse referred to the laser pulse (fig. 18).

In a wide field microscope with a high repetition rate laser, such as a Ti:Sa or YLF laser with frequency doubler, the gate delay can be controlled idependently of the laser pulse sequence. The acqusition time for each image is simply chosen to get a sufficient signal-to-noise ratio. If a laser with kHz repetition rate is used, the gate scan has to be synchronised with the laser, i.e. for each image a defined number of laser shots has to be acquired.

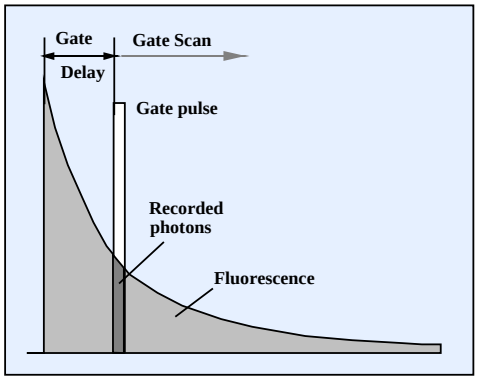

Fig. 18: Scanning a fluorescence decay function with the gate pulse

If a gated image intensifier is used in conjunction with a scanning microscope [20,33], the gate scan must be synchronised with the frame scan rate of the microscope.

A serious drawback of the gated image intensifier is the low counting efficiency. Due to the gating process, most of the photons collected from the sample are gated off. The counting efficiency is about the ratio of the gate width to the fluorescence lifetime and becomes more and more significant for shorter gate width. For a lifetime of 3.5 ns and a gate width of 200 ps [20] the efficiency is only 5.7 %. The F value [39], i.e. the ratio of the ideal to the actual SNR is 4.18.

The low efficiency must be compensated by a longer acqusition time with correspondingly more photobleaching in the sample. Although the multiple beam technique [48, 49] can be used to considerably reduce the acquisition time it does not really improve the detection efficiency.

The counting efficiency can be improved by using a very wide gate and measuring the fluorescence with only two gate delays. Single exponential decay constants can be derived from the intensities in the two time windows analog to multi-gate photon counting [50]. Since the measurements for the two gates have to be done one after another the counting efficiency of such a measurement is close to 0.5, i.e. by a factor of two less than for multi-gate photon counting.

In scanning microscope applications the gated image intensifier narrowly beats the multiple gate photon counting method for time resolution. The Pico Star System of La Vison [51] has a minimum gate width of 200 ps compared to 500 ps of the gated photon counting method [57,58]. However, the multiple gate photon counting method has a near-ideal counting efficiency, resulting in a correspondingly higher signal to noise ratio (SNR) for a given sample exposure.

In a scanning microscope the image intensifier cannot compete with time-correlated photon counting (TCSPC) imaging [67,68,69] in terms of time resolution and counting efficiency. TCSPC currently achieves 25 ps resolution and an F value and a counting efficiency close to one. TCSPC is even able to record in several wavelength intervals simultaneously [68] - a feature that pushes the efficiency of TCSPC beyond the theoretical limit of any single channel detection technique.

A gated image intensifier can be used for wide field illumination, for scanning with one-photon excitation and for scanning with two-photon excitation. However, it cannot be used in a confocal setup, and deep tissue two-photon images are blurred by scattering.

The realm of gated image intensifiers is clearly the wide field microscope [23]. If wide field illumination has to be used for whatever reason, there is currently no replacement for the image intensifiers.

Modulation Techniques

Modulation techniques use modulated light to excite the fluorescence. Referred to the excitation light, the fluorescence light has a phase shift and a reduced modulation degree (fig. 19). Both depend on the fluorescence lifetime and on the modulation frequency:

$$\tan \varphi_f = \omega \tau_f$$

$$M_f / M_{ex} = 1 / \mathrm{sqrt} (1 + \omega^2 \tau_f^{\,2})$$

ω angular frequency of modulation,
M_{ex} modulation of excitation, M_f modulation of fluorescence, φ_f phase lag of fluorescence,
τ_f fluorescence lifetime

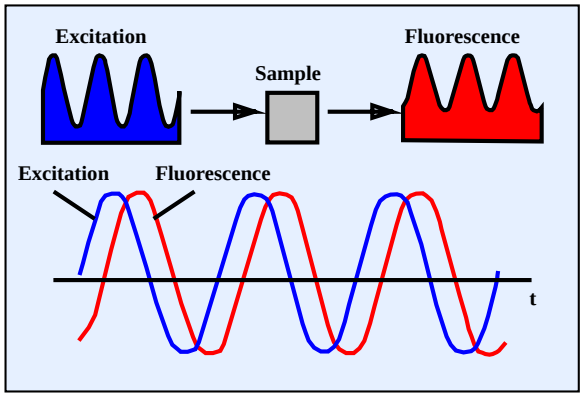

Fig. 19: Modulation technique

Both the phase and the modulation can be used to determine the fluorescence lifetime. However, phase measurements are much more accurate than measurements of the modulation degree. Therefore normally the phase is used for lifetime measurements. The optimum frequency depends on the lifetime and is

$$\omega = 1 / \tau_f \quad \text{or} \quad f = 1 / 2\Pi \tau_f$$

Since fluorescence lifetimes are of the order of nanoseconds or picoseconds a modulation frequency between 50 MHz and several 100 MHz is used. To resolve the components of multi-exponential decay functions phase measurements at different frequencies are necessary.

If a frequency between 100 MHz and 1 GHz is used the modulation method gives a time resolution in the ps range. For one-photon excitation the light source can be a modulated laser diode or a CW laser with an external modulator. For two-photon excitation a Ti:Sa laser is used and the phase is measured at the fundamental pulse frequency of the laser and at its harmonics.

Taking into consideration the high frequency, the wide amplitude range of the fluorescence signal and the low signal-to noise ratio the phase measurement is anything but simple. Consequently, there are several modifications of the method depending on different excitation sources, detectors and phase measurement methods.

Single Channel Modulation Techniques

The general principle of the single channel modulation technique is shown in fig. 20.

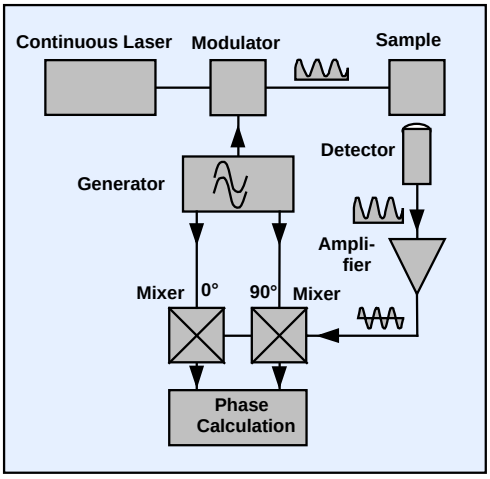

Fig. 20: Modulation technique

The light from the laser is modulated at a frequency in the range of 30 MHz to 1 GHz. The fluorescence light from the sample is detected by a PMT or a photodiode. The AC component of the detector signal is amplified and fed into two mixers that mix the signal with the modulation frequency at 0° and 90° phase shift. Mixing means actually a multiplication of the signals, therefore the outputs of the mixers deliver a DC component that represents the 0° and 90° components of the amplified detector signal. After low pass filtering the phase can be calculated from the mixer signals. The principle is analog to a dual-phase lock-in amplifier and often called lock-in detection [52,53].

The modulation technique can be used to record the fluorescence of several chromophores simultaneously in several parallel mixer systems. Several lasers which are modulated at different frequencies provide different excitation wavelengths. The emission of the sample is split into several wavelength ranges and detected by separate detectors. The detector signals are mixed with the modulation frequencies of the individual lasers in several parallel groups of mixers [52, 53].

Unfortunately high frequency mixers do not work well for DC output signals. Therefore, often a heterodyne principle, similar to that in a radio, is used (fig. 21). The detector signal and the modulation frequency are mixed with an oscillator frequency slightly different from the modulation frequency. The result are two signals at the difference frequency. The phase shift between the two signals is the same as between the detector signal and the modulation signal. Depending on the frequency difference, the output signals of the mixers are usually in the kHz range. Therefore they can directly be digitised. The results of the AD conversion are filtered and used for phase measurement. The advantage of direct digitising is that effective digital filtering algorithms can be applied and the phase can be determined via fast Fourier transform [54, 55].

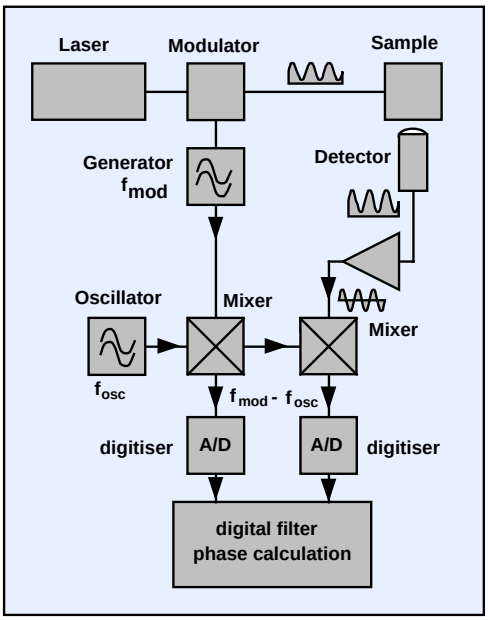

Fig. 21: Heterodyne principle

A phase fluorometer of this type can be built up by using a commercially available network analyser and a laser diode. The setup is very simple - unless you have to build the network analyser. The principle is shown in fig. 22. The network analyser runs a frequency sweep over a selectable frequency interval. The output signal of the network analyser drives a laser diode that is used to excite the sample. The detected fluorescence signal is fed back into the signal analyser. The measurement delivers the phase and the amplitude of the signal as a function of the frequency. The network analyser is even able to correct the results by using reference data recorded with a scattering solution in place of the sample.

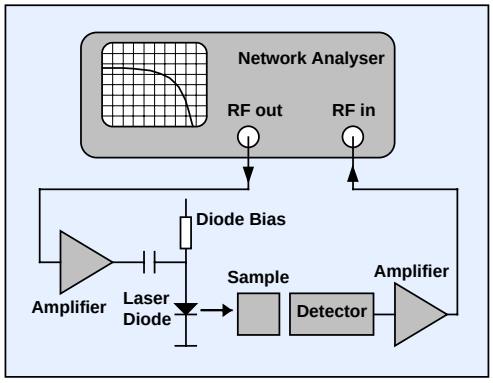

Fig. 22: Phase fluorometer with a network analyser

The mixers used in fig. 20 and 21 can be replaced with a modulated detector (fig. 23). A setup of this type has been used for lifetime imaging in a two-photon laser scanning microscope [54]. A commercially available frequency synthesiser generates the modulation frequency, the oscillator frequency and the difference of both with a high frequency and phase stability. Mixing is accomplished by modulating the gain in a photomultiplier. The mixed signal at the output of the PMT has a frequency of 25 kHz and is directly digitised. Further filtering and phase calculation is done digitally.

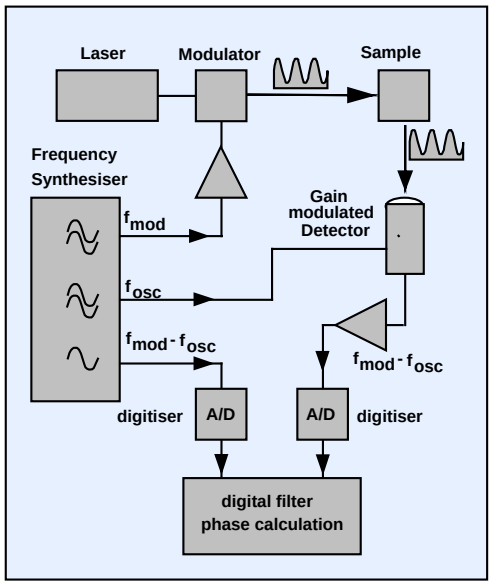

Fig. 23: Mixing by gain-modulating the detector

The benefit of the detector modulation is that the modulation frequency is not limited by the bandwidth of the gain system of the PMT. Therefore relatively high modulation frequencies can be used. The drawback is that the detector is a very poor mixer. This results in a poor efficiency of the detector gain modulation technique.

If a Ti:Sa laser is used in a modulation system, e.g. for two-photon excitation, the 80 MHz fundamental repetition frequency of the laser and its harmonics can be used as modulation frequency. Due to the short pulse width the spectrum of the laser modulation is actually a frequency comb that extends up to THz frequencies. By proper tuning of the frequency synthesiser, any of the harmonics of the fundamental repetition frequency within the detector bandwidth can be used for the phase measurement.

A heterodyne system with a Ti:Sa laser, two-photon excitation and modulated PMT delivered a lifetime accuracy of ± 300 ps for lifetimes between 2.4 and 4.2 ns [54]. This relatively poor accuracy is probably due to the short acquisition time of only 160 µs per pixel or 10 seconds for a 256 x 256 pixel image. Although the photon detection rate was estimated to be more than 10^8 photons/s - which is probably an overestimation - the accuracy is of the same order as for TCSPC imaging with 10^6 photons per second and the same acquisition time and pixel number.

The efficiency of the single channel modulation technique in terms of photon counts strongly depends on the operating conditions. Results of Monte-Carlo simulations of the efficiency for single-exponential decay are given in [39]. The simulations yield ‘F values’, i.e. the ratio of the ideal SNR to the SNR achieved by the investigated method.

For a setup with separate detector and mixer, sine-wave-modulated excitation, sine-wave mixing and 100% modulation of the excitation F was found to be 3.7. If the modulation is less than 100% a

fraction of unmodulated light is detected which contributes to the noise, but not to the phase measurement signal. The SNR drops dramatically for less than 75% modulation [39]. Interestingly, in the same setup 100 % square-wave modulation of the excitation gives an F = 1.2, and Dirac pulse excitation even F = 1.1. This is a strong argument to use pulsed lasers, i.e. Ti:Sa or diode lasers rather than modulating CW lasers.

For a gain-modulated detector the efficiency is much worse than for a detector and a separate mixer. The reason is that a gain modulated detector is a very bad mixer. True mixing means to multiply the detected signal with a sine wave, i.e. to invert the polarity of the signal for the negative half-period of the mixing signal. Of course, gain modulation at best means to change the gain between 100% and 0. Therefore a large fraction of the input signal remains unused, but contributes with its shot noise to the noise of the result. The F values for the modulated detector are around 4. That means, the technique needs 16 times more photons than techniques with a near-ideal F.

For extremely low light levels the situation can be even worse. A high gain detector, such as a PMT, delivers a train of extremely short current pulses rather than a continuous signal. The pulses are due to the detection of the randomly arriving photons. If this pulse train is fed to a phase measurement circuitry described above a phase signal is produced only for a short time after the detection of a photon. In the times between the phase detector is unable to deliver a reasonable signal. What then happens depends on the phase detection electronics or the equivalent software algorithm. A normal phase detector in the absence of a signal delivers a huge noise. This noise is averaged with the randomly appearing phase signals for the individual photons. The result is a dramatic drop of the signal-to-noise ratio for low photon rates.

For application with a scanning microscope it must be taken into regard that phase measurements are not compatible with the fast scanning speed of a state-of-the art laser scanning microscope. For the lock-in method the low pass filters must have time to settle, and the heterodyne method requires to record at least some periods of the difference frequency $f_{mod} - f_{osc}$. Therefore, minimum pixel dwell times are in the order of 40 to 160 µs. It is not clear whether a long pixel dwell time increases the photodamage in the sample. At least, the implementation of single channel modulation techniques in commercial scanning microscopes requires changes in the scan control of the microscope.

Another problem can arise for deep tissue imaging with a confocal or two-photon microscope. In this case the presumption that the time-domain response of the sample is a sum of exponentials is questionable. Scattered excitation light and broadening of the fluorescence decay functions by scattering remain unnoticed unless a continuous sweep over wide frequency interval is performed.

The conclusion is that the single channel modulation technique is not the best lifetime technique for scanning microscope applications. The true realm of the single channel modulation technique is in the infrared where no detectors with single photon sensitivity are available.

Modulated Image Intensifiers

The modulated image intensifier technique uses the same vacuum device as the gated image intensifier technique. However, the grid is driven by a sine wave or square wave signal rather than by a short gating pulse [55,56]. Modulation can also be achieved without a grid by modulating the voltage between the photocathode and the channel plate.

As for the gated image intensifier, the problem is the low conductivity of the photocathode. The time constant formed by the gate-cathode capacitance and the cathode resistance limits the modulation frequency and introduces lateral phase variation across the image. Furthermore, a

variable lateral field builds up in front of the photocathode that distorts the image and impairs the image resolution.

Modulating the voltage across the channel plate [55] has also been attempted. The drawback of this method is the heating of the channel plate due to dielectric losses and the low degree of modulation.

The microscope setup for a modulated image intensifier is shown in fig. 24. The setup is very similar to that for the gated image intensifier.

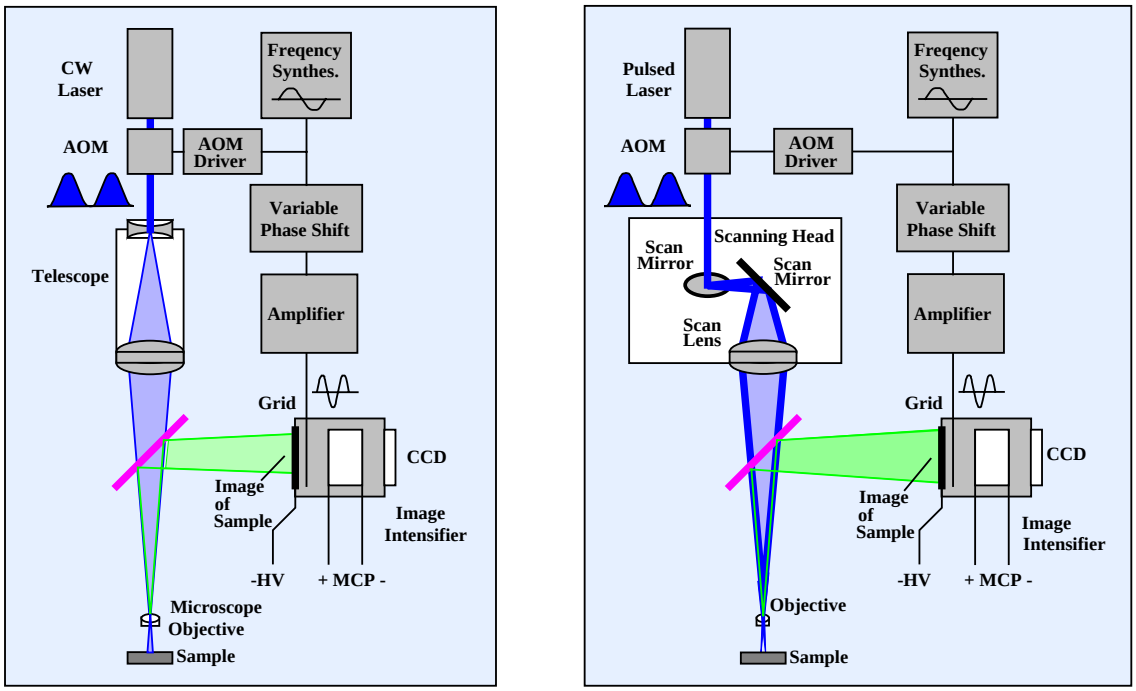

Fig. 24: Modulated image intensifier used at a wide field microscope (left) and at a scanning microscope (right)

A frequency synthesiser generates a modulation frequency which is typically in the range of 50 MHz to 500 MHz. This frequency is used to modulate the excitation light and the image intensifier. A variable phase shifter is used to change the phase relation between the modulation of the light source and the modulation of the image intensifier. From three images acquired at different phase shifts the phase of the fluorescence signal referred to the excitation can be calculated.

Instead of the phase shifter a heterodyne technique can be used. In this case the image intensifier is modulated with a slightly different frequency than the laser. This causes the phase between the two modulations to change continuously. If the difference frequency is a few Hz a sequence of images can be obtained for each period of the difference frequency [55]. The heterodyne technique requires a good frequency synthesiser that delivers the two modulation frequencies and the difference of both with high frequency and phase stability.

A single phase measurement at a fixed frequency allows to determine the time constant of a single exponential fluorescence decay function. To resolve the components of a multi-exponential decay measurements at different frequencies are required. Ideally, the modulation frequencies should be of the order of

$$f_{mod} = 1 / 2\Pi\tau_f \quad \text{with}$$

f_{mod} = Modulation Frequency, τ_f = Fluorescence decay time constant

At this frequency the change of the phase is at maximum for a given change of the decay time constant. For decay components below a few 100 ps the optimum frequency is around 1 GHz. Modulation frequencies of this order are almost impossible to achieve with standard image

intensifiers. The dielectric losses cause heat dissipation in the intensifier tube structures, and there is a considerable phase shift between different parts of the image area.

A modulated image intensifier can be used for one-photon and multi-photon fluorescence imaging with high repetition rate pulsed fs laser. The pulse train of the laser contains all harmonics of the fundamental repetition frequency. In the frequency domain the laser pulse train is actually a frequency comb that extends to THz range. Generally, by modulation the intensifier at the harmonics of the laser frequency a multi-frequency measurement can be accomplished [55,56]. A problem associated with this technique is that the gain modulation is nonlinear and therefore not ideally sinusoidal. Therefore the measurement signal obtained at a particular harmonic of the laser also contains a small fraction of higher harmonics.

A drawback of the image intensifier technique is that it cannot be used in a confocal scanning microscope. Therefore depth resolution can only be achieved by two-photon excitation with a fs laser [55]. Even then the spatial resolution is limited by scattering of the emission light in the sample. The multiple beam technique described for the gated image intensifier in [48,49] is also applicable for the modulated intensifier technique.

The efficiency of the modulated image intensifier in terms of photon exploitation has been investigated theoretically by Monte-Carlo simulations [39]. The F value, i.e. the SNR of an ideal measurement compared to the actually obtained SNR is 10 for sine-wave modulated exciatation and 4.3 for dirac modulation. That means the image intensifier needs 18.5 to 100 times more photons than techniques with perfect exploitation of the photons, e.g. time-correlated single photon counting.

The reason for the high F values is that the gain can only be modulated between 0 and 1. Ideal mixing requires gain modulation between -1 and +1. Thus the modulation depth is only 50%. The F values are even worse if the modulation of the gain in the intensifier tube is less than 50% - which is certainly the case if a device without a grid is used. Moreover, the modulation is an efficiency modulation rather than a gain modulation - the photoelectrons from the photocathode are either rejected or transmitted into the channel plate. Therefore the efficiency is worse than for a detector with a subsequent mixer.

The time resolution of the modulated image intensifier technique was reported to be down to a few 100 ps [55,56]. It is likely that much shorter lifetimes can be resolved if a sufficiently long acquisition time is used.

Generally the resolution of frequency domain techniques cannot directly be compared to the resolution of time domain methods. The decay times are calculated from the phase (i.e. from a part of the Fourier spectrum) of the fluorescence signal. This calculation includes reference measurements for a reference sample or zero decay time for each frequency. Correctly, the resolution of frequency domain methods should be compared with the resolution of time-domain methods with deconvolution of the decay data. Deconvolution of TCSPC data obtained with an MCP PMT resolves single exponential decay times down to a few ps.

Due to the low efficiency the modulated image intensifier technique it cannot be recommend as a lifetime method for laser scanning microscopes. However, the technique is applicable to wide field illumination. If wide field illumination has to be used for whatever reason there is currently no replacement for the gated and modulated image intensifier techniques.

Gated Photon Counters

As all photon counting techniques, gated photon counting uses a fast, high gain detector that is usually a PMT or a single photon avalanche photodiode. The single photon pulses from the detector are counted within one or more time intervals. Due to the moderate time resolution of the gating technique there are no special requirements to the transit time spread of the detector. However, the transit time distribution should not have a long tail, or bumps and prepulses or afterpulses and should be stable over the detection area. The principle of a gated photon counter with a single gate is shown in fig. 25.

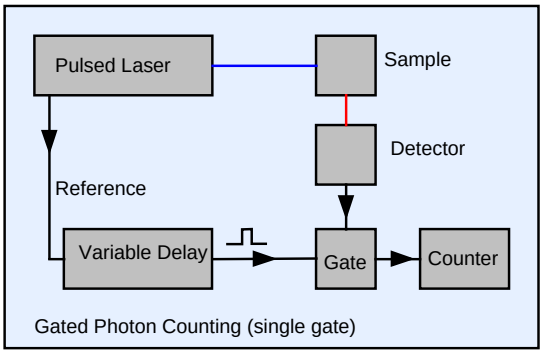

Fig. 25: Gated Photon counter with single gate

To record the shape of a fluorescence decay function the gate pulse can be scanned over the time interval of interest by a variable delay generator. This method yields a decay curve with as many points as the delay unit has delay steps. However, the majority of the photons is discarded by the gating. Thus, the counting efficiency is low and the F value is of the same order as for the gated image intensifier. Although ready-to use gated photon counters are available nobody seriously considers to use this technique for lifetime imaging.

A counting efficiency close to one can theoretically be achieved by a multiple gate architecture, fig. 26. The system contains several parallel counters with individual gates. The gates are controlled via separate gate delays and by separate gate pulse generators. If the measured decay curve is completely covered by subsequent gate pulses all detected photons are counted. Moreover, the parallel counter structure can be operated at extremely high count rates. Even for count rates of several MHz there is almost no counting loss due to the short dead time of the counters. The practical implementation of the method is described in [57, 58].

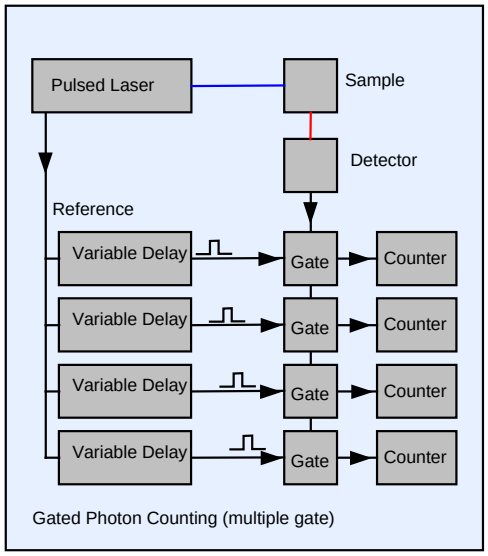

Fig. 26: Gated photon counting with several gates

Another benefit is that no special vacuum devices as for the image intensifier technique are required. The method immediately benefits from new detector developments, e.g. PMTs with high efficiency cathode materials [59,60].

Limitations of the method result from the relatively long gate duration and from the limited number of gate and counter channels. From the of signal-theory-point of view, the function of photon density versus time is heavily ‘undersampled’. In other words, the maximum frequency detectable in the signal spectrum is sampled less than 2 times per signal period. Undersampled signals cannot be reconstructed from the sample values without presumptions about the signal shape.

Fortunately, decay curves are either single exponentials or a sum of a few exponentials. Ideally, the lifetime of a single exponential decay can be calculated from the photons collected in only two time windows, see fig. 27. The optimum gate width was determined to be T = 2.5 τ_f [38]. It has been shown that the components of multi-exponential decay functions can be determined if the number of gates is increased [61].

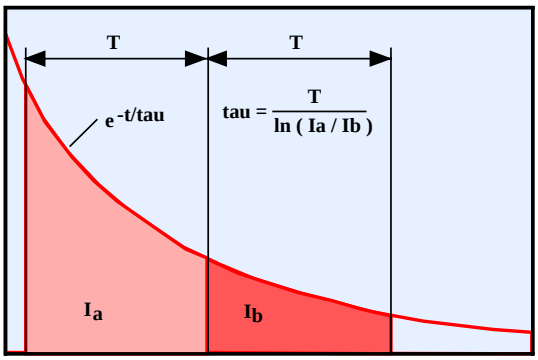

Fig. 27: Calculation of fluorescence lifetime from intensities in two time intervals, ideal IRF

However, practically the photons distribution is the convolution of the fluorescence decay function with the instrument response function (IRF), i.e. the excitation pulse shape, the detector TTS, the pulse dispersion in the optical system, and the effective shape of the gating pulse. The resulting fluorescence signal cannot be considered to be a sum of exponentials (fig. 28). To obtain the fluorescence lifetime from the intensity in two time windows these must be placed in a part of the fluorescence signal where the IRF has dropped below the noise level, i.e. in a region where the fluorescence signal is exponential. This, however, reduces the counting efficiency by discarding the most intense portion of the signal. Practically it is probably better to tolerate some error in the lifetime calculation and to calibrate the system by using known fluorescence lifetimes. However, for double- or multi-exponential decay functions a calibration appears difficult if not impossible.

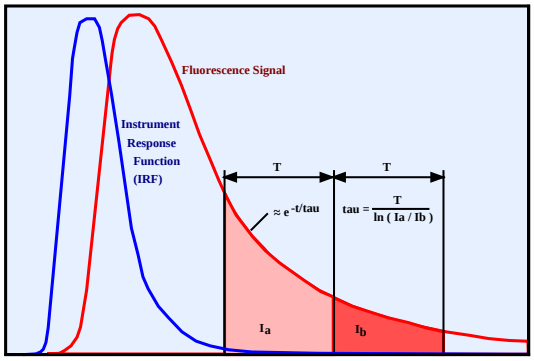

Fig. 28: Calculation of fluorescence lifetime from intensities in two time intervals, real IRF

The shortest gate width that has practically been used is of the order of 500 ps. Although lifetimes down to 70 ps have been measured with reasonable accuracy it is difficult to measure lifetimes below 200 ps. Double exponential decay functions of FRET systems with a fast component of 100 to 300 ps probably cannot be resolved.

Practical devices based on multi-gate photon counting work with a direct readout of the counters after the acquisition of each pixel of the image [57]. This sets a lower limit to the pixel dwell time in the 10 us range. Consequently, the maximum scan speed of a laser scanning microscope cannot be exploited. It is not clear whether this increases the photobleaching of the sample via accumulation of triplet states or heat concentration in the scanned spot. The problem - if it exists - could easily be overcome by implementing a memory that accumulates the results in memory locations according to the x,y location of the laser spot in the scanning area.

For samples containing different chromophores the counting efficiency and the amount of information in the data can be improved by recording the fluorescence in several wavelength channels simultaneously. Steady-state multi-wavelength imaging has been successfully used to separate different chromophores in stead-state images [13]. The gated photon counting technique basically can be used with several detectors if the number of gate and counter channels is increased. Several gates can be driven by the same delay and gate pulse generator so that the increase of system complexity is less than proportional. Although a multi-wavelength gated SPC system has not become known yet it could improve the selectivity for different chromophores considerably.

Theoretical investigation of the efficiency [39] delivers an F value of 1.5 for two gates of a width of 2.5 τ. For 8 gates with unequal width F = 1.1 can be achieved. However, practically τ is unknown and varies throughout the image so that the gate width is usually not optimal. Furthermore, the first

part of the signal can probably not be used because it is convoluted with the system response. Assuming a loss of a factor of two in the number of counted photons the +method ends up at F = 1.5 to 2.1 which is much better than for the image intensifiers and noticeably better than sine-wave modulation techniques.

Acquisition times for biological samples stained with highly fluorescent dyes are in the range 10 to 100 seconds [58,11]. Generally the acquisition times for comparable lifetime accuracy should be expected in the same range as for TCSPC imaging (see below) unless count rates exceeding 5 MHz are available. As for TCSPC imaging, the acquisition time can be reduced by decreasing the number of pixels of the scan.

Multi-gate photon counting has its merits in applications that require to record lifetimes in the range of a few ns at high count rate and with short acquisition times. Typical applications are lifetime imaging with marker dyes for Ca++, Na+, O-- or other parameters within cells and tissue [11b]. Probing of DNA and RNA by the lifetime change of SYTO13 is described in [11, 11a].

Time-Correlated Single Photon Counting (TCSPC)

Time-Correlated Single Photon Counting is based on the detection of single photons of a periodical light signal, the measurement of the detection times of the individual photons and the reconstruction of the waveform from the individual time measurements [62, 63]. The principle is shown in fig. 29.

The fluorescence is excited by a pulsed laser with a repetition rate of typically 80 MHz. The fluorescence photons are detected by a fast PMT, MCP or a single photon avalanche photodiode. For precision measurements these detectors allow count rates of the order of a few MHz, i.e. much less than the laser repetition rate. The TCSPC method makes use of the fact that the detection of several photons in one laser period is small enough to be neglected. When a photon is detected the time of the corresponding detector pulse in the laser pulse sequence is measured. The measured times are used to address a histogram memory in which the photons are accumulated. After acquiring a large number of photons the photon density versus time builds up in the memory.

The method may look circumstantial at first glance, but it has some striking benefits - a near-ideal counting efficiency and an ultra-high time resolution.

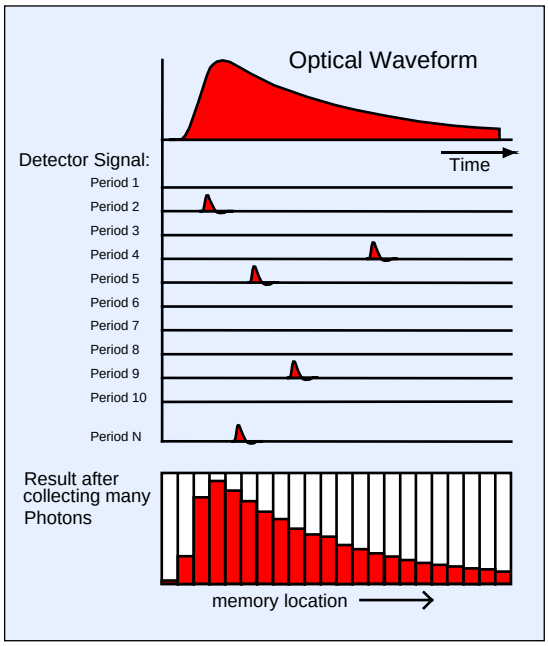

Fig. 29: Time-correlated single photon counting

As long as the count rate is not so high that the conversion time of the time measurement and histogramming procedure becomes noticeable there is no loss of photons. The F value describing the ratio of the ideal SNR to the actually obtained SNR is < 1.1 [38,39].

The resolution is limited by the transit time spread in the detector, by the timing accuracy of the discriminator that receives the detector pulses and by the accuracy of the time measurement. With an MCP-PMT the width of the instrument response function is of the order of 25 to 30 ps. The width of the time channels of the histogram can be made less than 1 ps [63]. Therefore, the instrument response function is sufficiently sampled to determine lifetimes down to a few ps.

The TCSPC technique is often believed to be extremely slow and unable to reach short acquisition times. This ill reputation comes from older NIM systems used in conjunction with low repetition rate light sources which are indeed not applicable for time-resolved imaging.

However, high count rate techniques exist [64] since the late 80s. An early - probably the first - implementation of TCSPC in a microscope is described in [65].

State-of-the-art TCSPC devices use a new conversion principle and achieve count rates of several 10^6 photons per seconds [63]. A system with four parallel TCSPC channels and 20 MHz useful count rate is described in [66]. The system was used in a slow-scan setup for optical tomography and can be combined with a multi-detector technique [63,66]. Although a combination with a scanning microscope has not become known yet the system is basically able to record images in up to 32 detector channels with slow scan rates at count rates comparable to multi-gate photon counting [57].

TCSPC Imaging

TCSPC Imaging is an advanced TCSPC technique used in conjunction with scanning microscopes. The method builds up a three-dimensional histogram of the photon number over the time and the coordinates of the scan area. The principle is shown in figure 30. The recording electronics consists of a time measurement channel, a scanning interface, and a large histogram memory.

The time measurement channel contains the usual TCSPC building blocks. Two constant fraction discriminators, CFD, receive the single photon pulses from the detector and the reference pulses from the laser. The time-to-amplitude converter, TAC, measures the time from the detection of a photon to the next laser pulse. This ‘reversed start-stop‘ principle is the key to the processing of high laser repetition rates. The analog-digital converter, ADC, converts the TAC output voltage into an address for the memory.

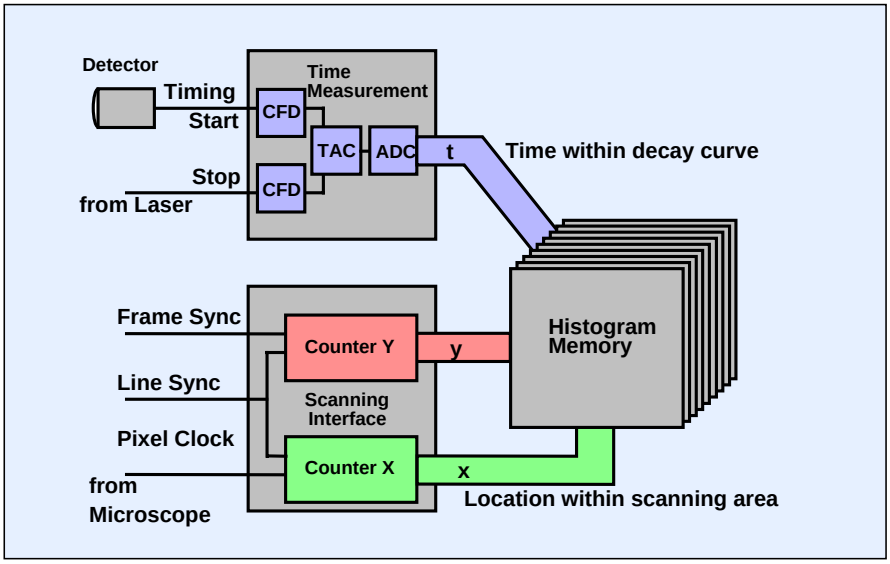

Fig. 30: TCSPC Imaging

The scanning interface is a system of counters. It receives the scan control pulses from the microscope and determines the current position of the laser beam in the scanning area.

When a photon is detected the device determines the time, t, within the fluorescence decay curve and the location of the laser spot within the scanning area, x, y. These values are used to address the histogram memory. Consequently, in the memory the photon distribution versus t, x, and y builds up. The result can be interpreted as a stack of images for different times after the excitation pulse or as an array of pixels containing a complete fluorescence decay function each.

The implementation of TCSPC imaging into Zeiss microscopes is described in [67-69]. The described instrument consist of a Zeiss LSM-510 NLO Laser scanning microscope, a femtosecond Ti:Sa laser, a fast PMT, and a Becker & Hickl SPC-730 TCSPC imaging module [63]. The setup is shown in fig. 31.

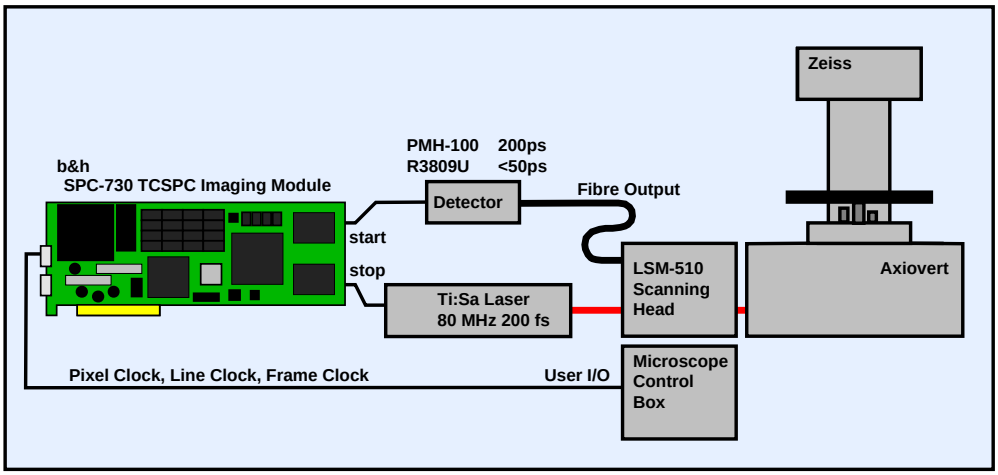

Fig. 31: Setup of the lifetime microscope

The setup does not require any changes in the microscope or in the associated control software. The fibre output option of the LSM-510 scanning head is used to feed the detected light into the photomultiplier. Depending on the required resolution either a PMH-100 detector head of Becker & Hickl or an R3809U MCP-PMT of Hamamatsu is used. For each photon, the detector delivers a start pulse to the SPC-730 TCSPC imaging module. The stop pulse for the time measurement is obtained from the monitor diode of the laser. The recording in the SPC-730 TCSPC module is synchronised with the scanning via the Pixel Clock, Line Clock and Frame Clock signals from the control box of the microscope.

The system response for a Hamamatsu R3809U MCP is shown in fig. 32. The instrument response width is 30 ps for an MCP supply voltage of -3000 V.

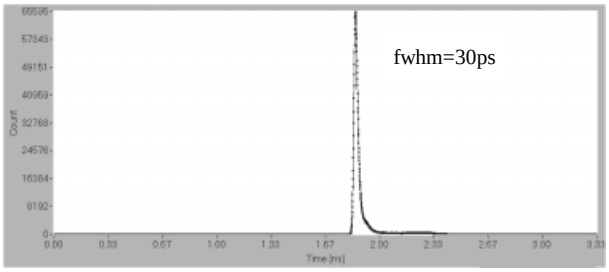

Fig 32: Instrument response for the R3809U-50 MCP

Usually, deconvolution of the measured fluorescence decay from the system response delivers decay at least times 10 time shorter than the system response, i.e. less than 3 ps. Deconvolution requires to record the instrument response function (IRF), which is simple in a one-photon microscope. However, in a two-photon microscope the IRF is difficult to record because the excitation wavelength is blocked by filters, or detectors are used which are insensitive at the excitation wavelength. Furthermore, the sample is excited by a two-photon process while the detector sees the response via one-photon photoemission. For standard applications a 'best guess' system response can be calculated from the rising edge of the fluorescence decay functions themselves. The shortest lifetime that can reasonably be determined this way is in the range of the IRF width, i.e. 20 to 30 ps. For precision measurements an ultra-short fluorescence or a nonlinear crystal can be used to record the IRF.

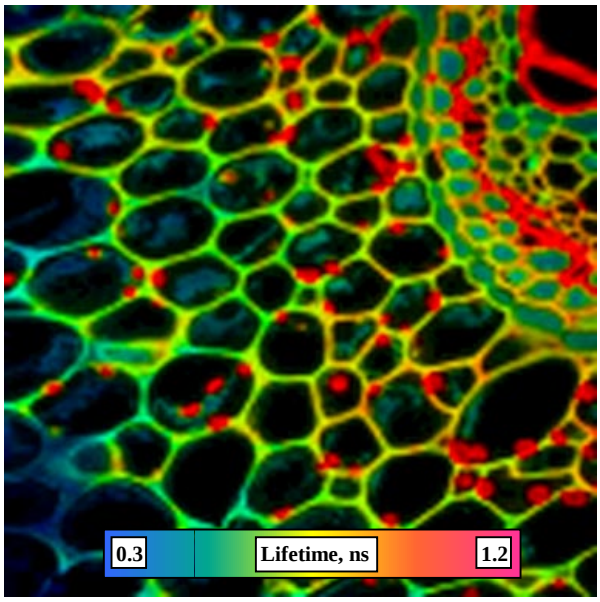

Fig. 33: Lifetime image of a sample stained with three different dyes (Leica TCS SP2, SPC-730)

Lifetime images obtained by TCSPC imaging are

presented in [67-75]. An example is shown in fig. 33. The sample is stained with three different dyes which are clearly distinguished in the lifetime image.

An application to FRET imaging (after [68]) is shown in figure 34.

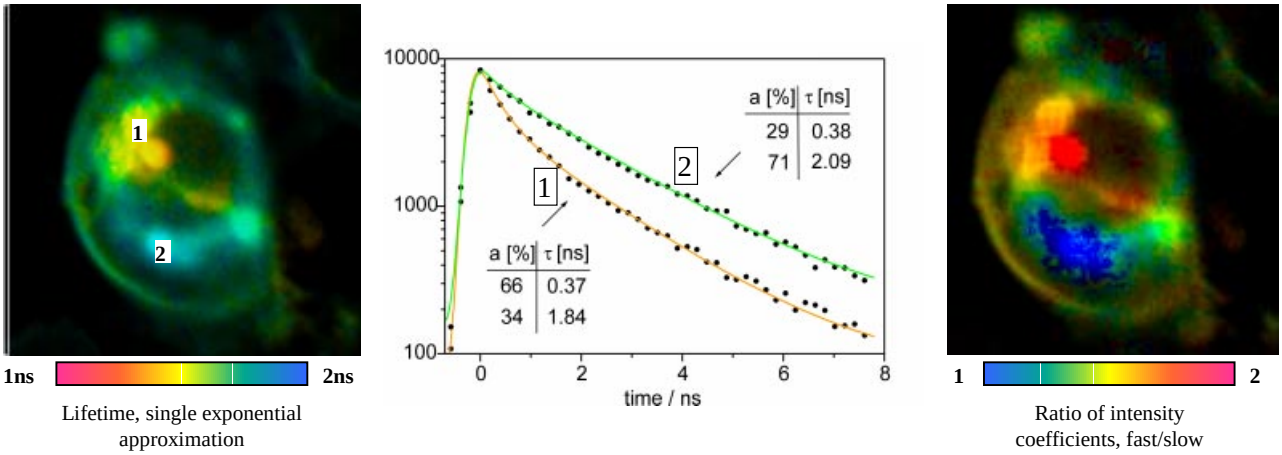

Fig. 34: HEK cell containing CFP and YFP in the α and β subunits of the sodium channels.
Left: Lifetime image of donor, CFP, centre: Decay curves of selected pixels, right: FRET image showing ratio of intensity coefficients of quenched and unquenched fluorescence components
Data from [68], Zeiss LSM-510, Becker & Hickl SPC-730

The sample is an HEK cell containing CFP and YFP in the α and β subunits of the sodium channels. Since the emission spectrum of CFP overlaps the absorption spectrum of YFP FRET is expected in regions where the subunits are close together. Fig. 34, left, shows a lifetime image of the donor, CFP, obtained from a single exponential fit through the decay functions in the individual pixels.

Fig. 34, centre, shows decay curves of two selected pixels from the yellow (short lifetime) and blue (long lifetime) area of the lifetime image. Double exponential decay analysis yields two decay components of about 380 ps and 1.8 to 2 ns throughout the image. However, the intensity coefficients, a, differ considerably in different parts of the cell. Assuming that the lifetime components belong to the quenched and unquenched donor molecules the ratio of the intensity coefficients, a_{fast} / $a_{slow,}$ should represent the ratio of the number of quenched and unquenched CFP molecules. Therefore the ratio of the coefficients can be used as a measure for the FRET intensity. Fig. 34, right shows a FRET image displaying the number of photons as brightness and a_{fast}/a_{slow} as colour.

Multi Wavelength TCSPC Imaging

For samples containing different chromophores the counting efficiency and the amount of information in the data can be increased by recording the fluorescence in several wavelength channels simultaneously. Multi-wavelength imaging has been successfully used to separate different chromophores in stead-state images [13]. TCSPC detection of single molecules in four wavelength channels considerably improves the selectivity for different molecules [17].

TCSPC imaging can be combined with a multidetector technique [63,66,76,77] and be used to record the photon density over time, wavelength and the coordinates of the scanning area [72]. The principle of the multi-detector technique is shown in fig. 35.

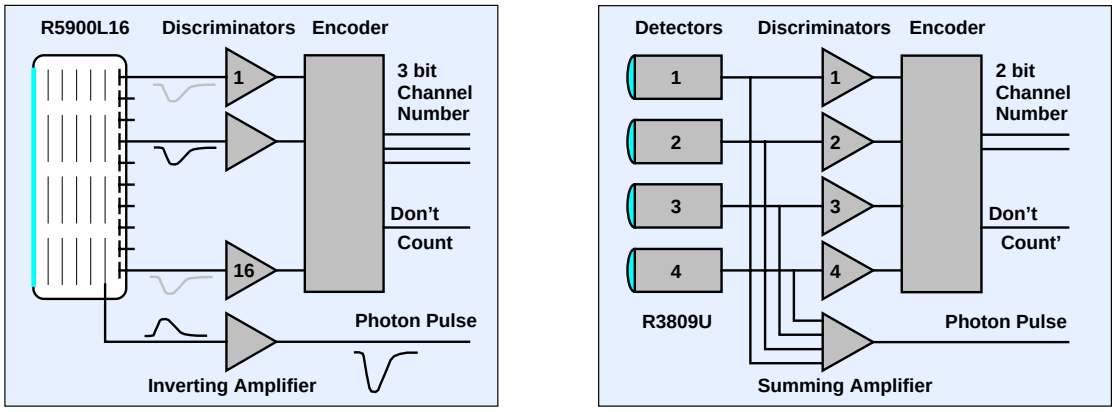

Fig. 35: Multi-detector technique for TCSPC. Left: Multichannel PMT, Right: Individual PMTs

The technique works both with a multichannel PMT [72a,77] and with several individual PMTs or MCPs [72b,66,76]. It makes use of the fact that the detection of several photons in different detector channels in one laser period is unlikely. Therefore, the single photon pulses from all detector channels can be combined into a common photon pulse line and send through the normal time measurement procedure of the TCSPC module. The output of each PMT channel is connected to a discriminator. If the channel detects a photon the corresponding discriminator responds and sends a pulse to the subsequent encoding logic. The encoder delivers the number of the PMT channel that detected the photon. The channel number is used as an additional dimension in the multi-dimensional histogramming process of the TCSPC imaging technique.

The recording electronics for multi-wavelength TCSPC imaging consists of a time measurement channel, a scanning interface, a detector channel register, and a histogram memory (fig. 36).

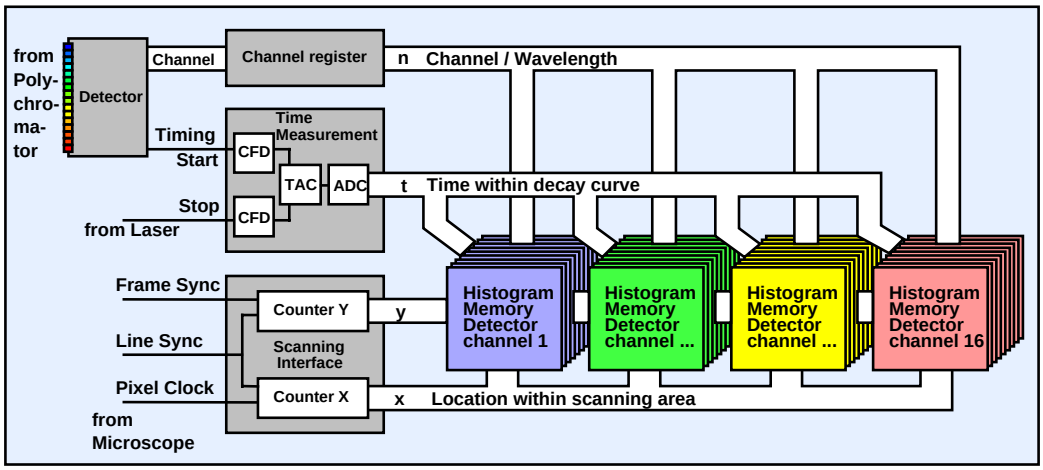

Fig. 36: Multi-wavelength TCSPC lifetime imaging

For each photon, the time measurement channel determines the detection time (t) referred to the next laser pulse. The scanning interface determines the current location (x and y) of the laser spot in the scanning area. Synchronously with the detection of a photon, the detector channel number (n) for the current photon is read into the detector channel register. If a polychromator is used in front of the detector, n represents the wavelength of the detected photon.
The obtained values for t, x, y and n are then used to address the histogram memory. Thus, in the memory the distribution of the photons over time, wavelength, and the image coordinates builds up. The result is a four-dimensional data array that can be interpreted as a set of image stacks for

different wavelengths. Each stack contains a number of images for subsequent times after the excitation pulse.

Fig. 37 shows a HEK 293 cell expressing a hybrid protein in which the cyan (CFP) and yellow (YFP) shifted mutants of the green fluorescent protein are linked together by a short amino acid chain. The setup used for this measurement [72a] consisted of a laser scanning microscope (LSM-510, Zeiss), a polychromator (250is, Chromex), and a 16 channel TCSPC detector head [77] connected to an SPC-730 TCSPC imaging module [63]. The setup recorded the wavelength range from 410 nm to 635 nm in 16 wavelength channels, covering the emission bands of CFP and YFP. The image below was obtained by summing the photons from all time channels of the CFP fluorescence.

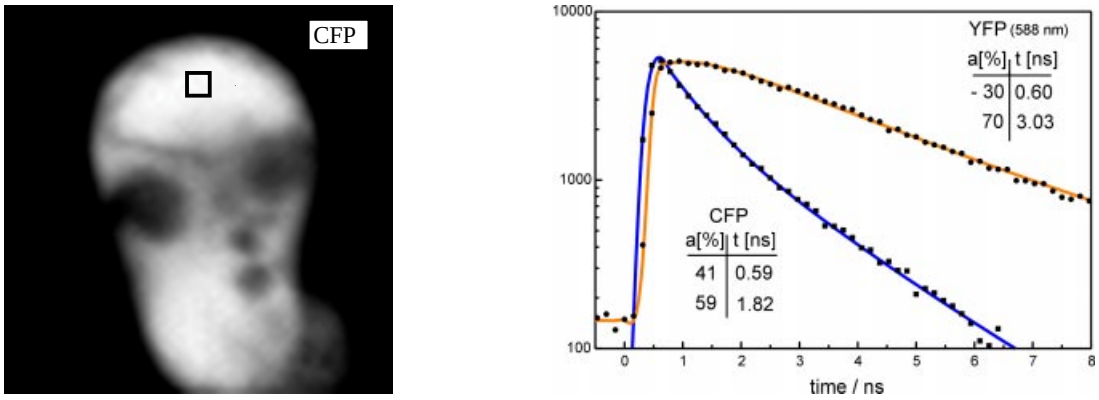

Fig. 37: HEK 293 cell expressing a CFP-YFP hybrid protein
Left: Intensity image of CFP. Right: Fluorescence decay curves of CFP and YFP in a selected region (square).

Fluorescence decay analysis in a selected region (small square) reveals a double-exponential decay both for CFP and YFP. The intensity coefficient of the fast component is positive for CFP and negative for YFP, indicating that energy is transferred from CFP to YFP. In Fig. 38 the intensity is represented by the brightness, the ratio of the coefficients by the colour of a pixel. The results are shown for the CFP and the YFP fluorescence.

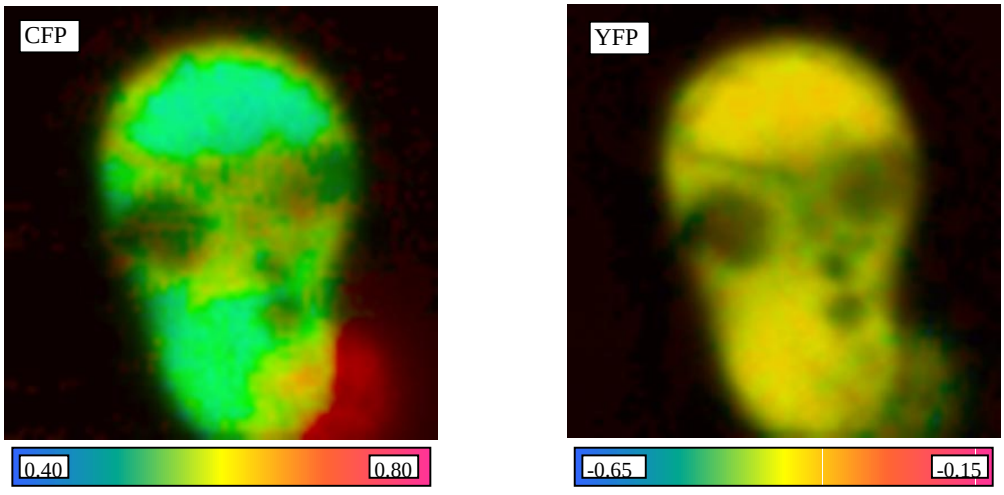

Fig. 38: FRET images for CFP (left) and YFP (right) of a HEK cell expressing a hybrid protein in which CFP and YFP are linked together by a short peptide. The brightness represents the intensity, the colour the ratio of the amplitudes of the fast and slow decay components. From [72a]

Features of the TCSPC imaging techniques

It should be pointed out that neither single wavelength nor multi-wavelength TCSPC imaging use any time gating or wavelength scanning. Therefore, both techniques yield a near-perfect counting efficiency and a maximum signal to noise ratio for a given acquisition time. Due to the short dead time of the TCSPC imaging electronics (125 to 180 ns) [63] there is almost no loss of photons for count rates up to a few 10^5/s as they are typical for cell imaging.

The time resolution of the TCSPC techniques is given by the transit time spread in the detector. A system response of only 25 ps FWHM is achieved with MCP PMTs. In conjunction with a minimum time channel width of the TCSPC modules of less than 820 fs [63] lifetimes down to a few ps can be measured.

No special vacuum devices as for the image intensifier technique are required. The method immediately benefits from new detector developments, e.g. ultra-fast MCP PMTs or new high efficiency cathode materials.

Implementing TCSPC imaging into a laser scanning microscope requires no more changes than attaching a fast detector to the microscope. In most microscopes this is possible either via a fibre output or via the non-descanned port.

TCSPC imaging works at the full scan rate of the laser microscope, i.e. with pixel dwell times of order of 1 µs. Due to the synchronisation via the scan control pulses the zoom and image rotation functions of the microscope can be used also for lifetime imaging.

Currently available TCSPC imaging devices have a limited memory space. Therefore, a tradeoff between the number of pixels, the number of time channels and the number of detector channels has to be made. However, with the introduction of the SPC-830 module of bh memory space is not longer a severe constraint. Some combinations of image size, and number of time and wavelength channels for the SPC-830 are given in the table below [63].

Detector Channels	Resolution x,y	Time Channels	Min. Time Channel Width (ps)
1	2048 x 2048	4	50
1	1024 x 1024	16	12.5
1	512 x 512	64	3.125
1	256 x 256	256	0.8
1	128 x 128	1024	0.8
4	1024 x 1024	4	50
4	512 x 512	16	12.5
4	256 x 256	64	3.125
4	128 x 128	256	0.8
16	512 x 512	4	50
16	256 x 256	16	12.5
16	128 x 128	64	3.125
16	64 x 64	256	0.8

Parallel operation of two modules connected to the same detector can be used to simultaneously obtain images with high pixels resolution and moderate time resolution and images with moderate pixel resolution and high time resolution. Although no such system has become known yet the implementation with current TCSPC modules is straightforward.

The maximum photon count rate of the TCSPC technique is limited by the time required to measure the time of a detected photon and to store it in the histogram memory. This ‘dead time’ is of the order of 125 to 180 ns for state-of-the art devices. Becker & Hickl define a ‘maximum useful count rate’ which means the **recorded** photon rate at which 50% of the photons are lost in the dead time [63]. Maximum useful count rates are in the range of 3 to 4 MHz. The counting efficiency and

the ‘figure of merit’ [39] as a function of the detector count rate for different techniques are shown in fig. 38. The values for the image intensifiers and single channel nmodulation techniques were taken from [39], the value for multi-gate photon counting from [81].

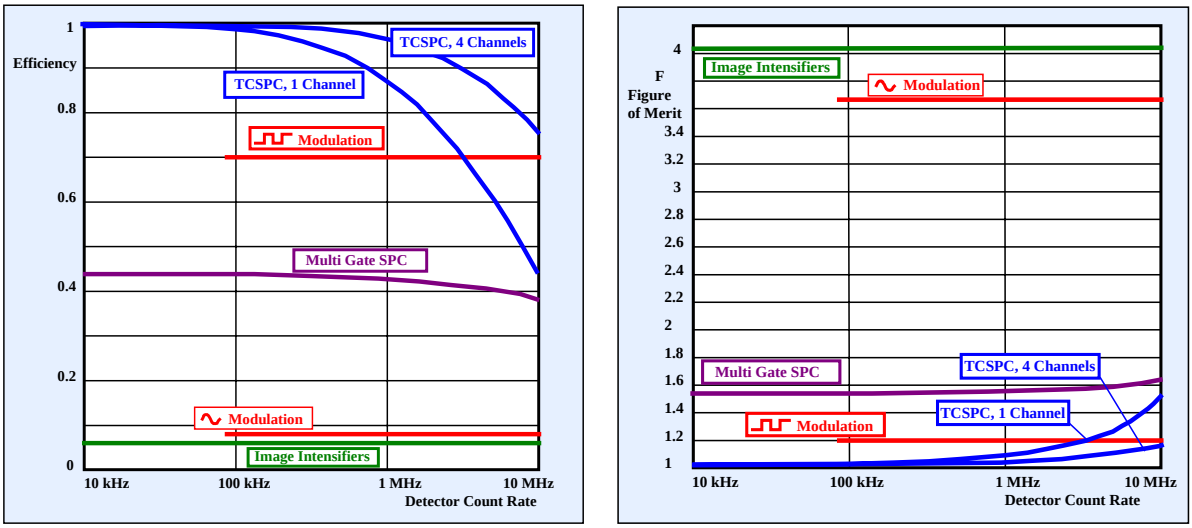

Fig. 38: Counting efficiency and figure of merit F of TCSPC imaging compared to other techniques
F is the ratio of theoretical SNR to obtained SNR, F=1 means ideal SNR

Surprisingly, TCSPC imaging beats the other methods even for detector count rates of the order of 5 to 10 MHz.

It is unlikely that such high count rates can be obtained from living cells. Anyway, a count rate above 5 MHz imposes overload problems to most detectors. Although traditional PMTs still work at 10 MHz the timing performance may not longer meet the high standard of the TCSPC method. MCP PMTs, i.e. the fastest detectors for TCSPC, are clearly overloaded above 1 MHz. If a system is to be operated at extremely high count rates the solution is the multidetector technique. If the light is split into several detection channels the load for the individual detectors is reduced.

Another solution is to operate several TCSPC modules with individual detectors in parallel. Although no such application has become known yet the implementation is straightforward. The Becker & Hickl TCSPCs are designed to work in packages of up to four devices [63].

The acquisition time for TCSPC lifetime measurements can vary in a wide range. In vivo lifetime measurements at the human ocular fundus in conjunction with an ophthalmologic scanner delivered single exponential lifetimes for an array of 128x128 pixels within a few seconds [75, 75b]. On the other hand, for the double exponential decay data of FRET measurements acquisition times from 5 to 30 minutes were used [68].

In practice the acquisition time depends on the required lifetime accuracy, on the number of lifetime components to be resolved, on the number of pixels and wavelength channels and on the count rate that can be obtained from the sample without photobleaching or photodamage. Fig. 39 shows the acquisition time as a function of the product of the number of pixels and the number of wavelength channels. The left diagram is for a high count rate of 10^6 /s. Count rates of this order can be obtained by one-photon excitation from cells containing high chromophore concentrations. For two-photon excitation a count rate of 10^6 /s requires extremely stable samples stained with very efficient chromophores.

The right diagram is for a very low count rate of 10^4 /s. Count rates of this order are typical for autofluorescence of cells and tissue and for samples with low photostability. An HEK cell

containing CFP and YFP measured by two-photon excitation with 150 fs pulses at 820 nm [68] delivered only 10^4 photons/s. Nevertheless, it photobleached to 50% intensity within 10 minutes.

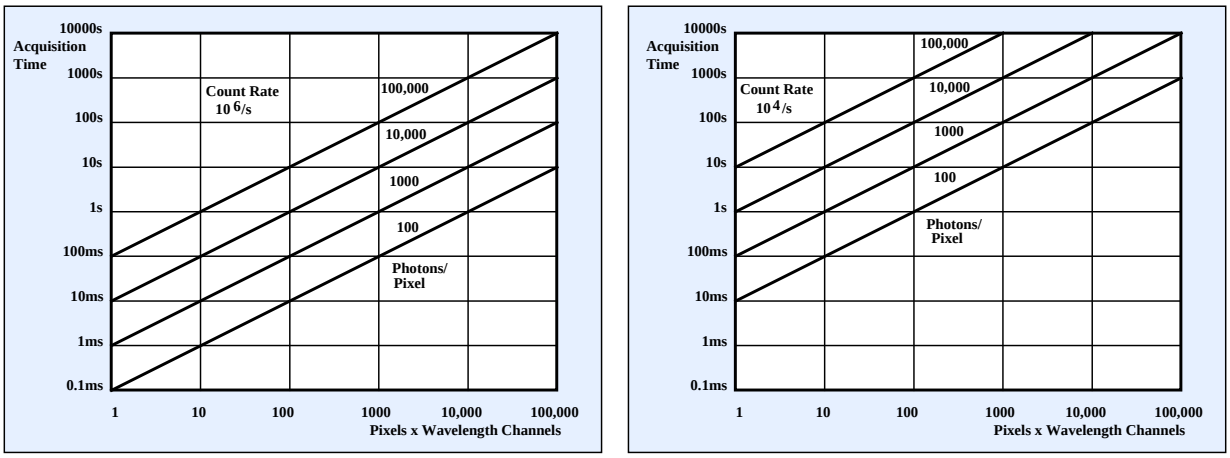

Fig. 39: Acquisition times for a count rate of 10^6 /s (left) and 10^4 /s (right) for different numbers of photons per pixel. Photons per pixel range from 100 for rough single exponential decay mapping to 10^5 for precision double exponential decay analysis.

Fig. 39 shows that relatively long acquisition times must be expected, particularly for large numbers of pixels and precision measurements of samples at a low count rate. However, it should be pointed out that long acquisition times are not a special feature of TCSPC imaging - they simply result from the fact that much more photons per pixel are required to determine the lifetime than to record the intensity.

Shorter acquisition times can be achieved if the scanning area is confined to a few pixels or only one pixel is measured. For single pixels the acquisition time can be in the ms or sub-ms range. That makes it possible to investigate diffusion processes by monitoring the lifetime change in a single pixel. Even fast FRET measurements appear feasible. FRET requires to resolve the components of a double exponential decay function. This requires about 10,000 photons which can be obtained in 10 ms.

Even if the emission intensity of biological samples is limited there is probably still some potential to increase the count rate by improving the detection efficiency. The transmission band of filters used to select the emission from a particular chromophore are often narrower than the emission band. Optimising the filters can easily yield a factor of two in sensitivity. Moreover, in a normal microscope the photons are collected from one side of the sample only. The 4Pi technique [37] collects the fluorescence from both sides and therefore gives a factor of two improvement in collection efficiency.

In cases where the full diffraction-limited resolution of the objective is not required the count rate can probably be increased by increasing the excited sample volume. Photobleaching is reported to be highly nonlinear, therefore the larger volume allows to use more excitation power and consequently to get more photons [43,45]. By introducing defined distortions into the wavefront of the excitation path or by under-illuminating the aperture of the objective the excited volume can be increased without impairing the photon collection efficiency.

Recently new photomultiplier cathodes with a 3-fold improved sensitivity compared to traditional bialkali and multialkali cathodes became available. Fast PMTs and MCPs with the new cathodes have an IRF width of 300 ps and 100 ps respectively [59,60].

Other TCSPC Techniques

Application of TCSPC to diffusion in cells

Diffusion constants in cells are usually determined by fluorescence correlation (FCS) techniques. Recording an FCS function requires to detect the fluorescence intensity in a fixed spot of the sample and to calculate the autocorrelation function of the intensity or of the photon detection times [14,15,16]. Although FCS is not an imaging technique it is often used in combination with imaging to define the location in a cell where an FCS measurement has to be run.

Generally, the TCSPC technique is not only able to record time-resolved images in laser scanning microscopes, but also to recorded FCS data. An FCS measurement can even be combined with a single point lifetime measurement. The multi-detector technique described above for TCSPC imaging is also available for FCS measurements. With the introduction of the SPC-830 it is not longer necessary to use independent modules for imaging and FCS. The SPC-830 works for imaging and FCS recording as well.

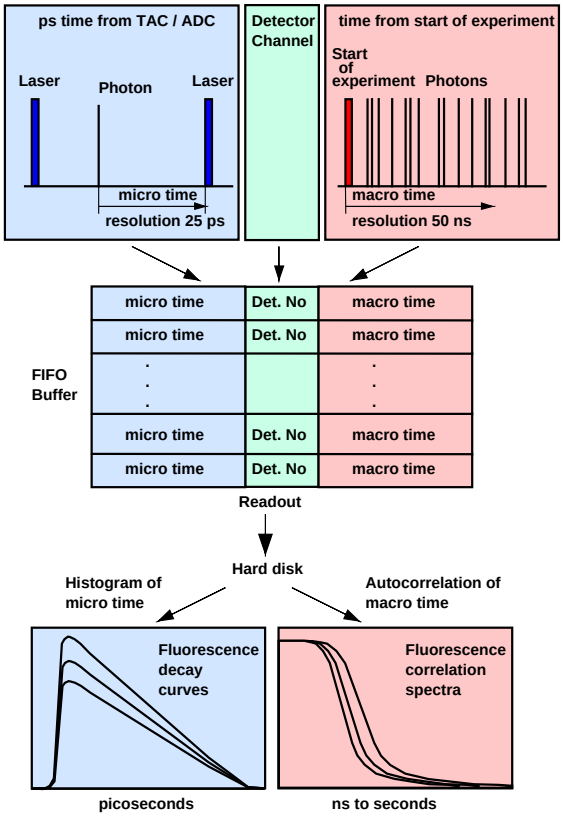

Fig. 40: Combined liftime / FCS data acquisition by TCSPC

FCS data recording does not build up histograms as the TCSPC imaging techniques do. Instead, it records the full information about each photon. Each entry contains the time of the photon in the laser pulse sequence, the time from the start of the experiment, and the detector channel. The data structure is shown in Fig. 40. For each detector an individual correlation spectrum and a fluorescence decay curve can be calculated. An instrument like this was used to detect and identify single molecules on a substrate. By using four wavelength channels and a piezo scanning stage different molecules could be identified in a time of the order of 1 ms [17]. Moreover, data from different detectors can be cross-correlated. By detecting different chromophores in different wavelength intervals cross-correlation can show whether the molecules of both chromophores and the associated protein structures are linked or diffuse independently.

TCSPC Wide Field Imaging

TCSPC can be used for wide field imaging if a special detector is used. The detector consists of the usual photocathode, a microchannel plate and a delay line system or a four-element anode system at the output. By measuring the delay of the output pulses at the ends of the delay lines or the charge distribution at the four anode sectors the location of a photon can be determined, see fig. 41.

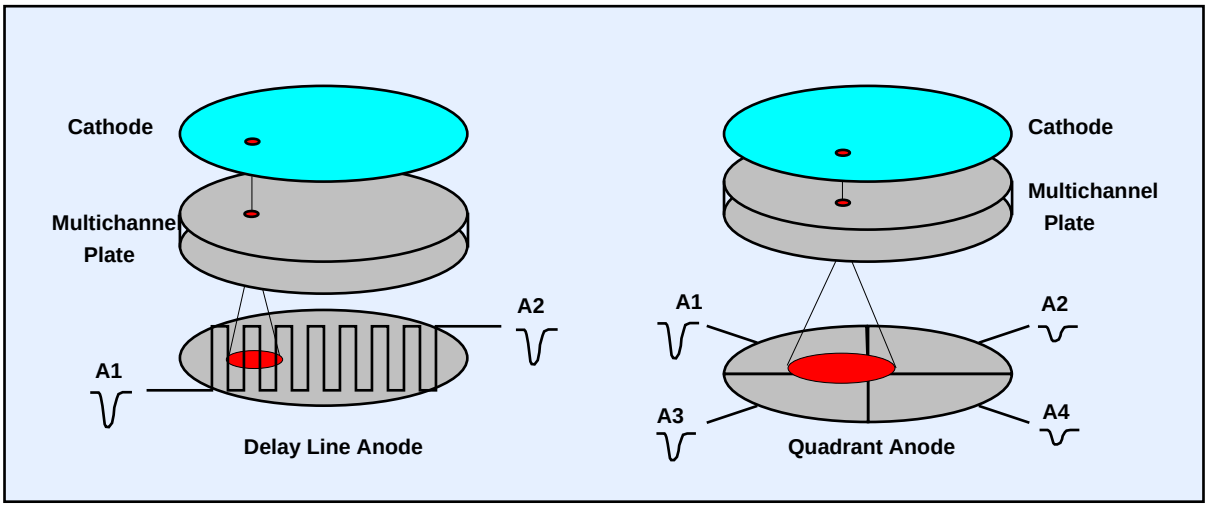

Fig 41 : Wide field detectors for TCSPC

Wide-field TCSPC imaging requires several TCSPC channels or one TCSPC channel with four low noise charge detection channels. The technique features high counting efficiency and relatively good time resolution. Because additional signal processing is needed to obtain the position of a photon it is difficult to reach high count rates. The most severe drawback is that the technique depends on complex detectors that are not commonly available.

Comparison of Signal Processing Techniques

A comparison of the different lifetime techniques is given below.

The figure of merit, F, was taken from [39]. Small F values indicate high efficiency. For multi-wavelength techniques it was assumed that two chromophores are measured which give approximately the same count rates. Therefore, the efficiency, E, increases by a factor of 2 and F is reduced by a factor of 1.4. The resulting F can be smaller and E greater than one because the values are referred to a single detector measurement with ideal SNR.

For the time resolution of the gated image intensifier and the TCSPC technique it was assumed that lifetimes down to 1/10 of the instrument response width can be de-convoluted, which is certainly a conservative assumption. The resolutions given for the modulation techniques are the practically obtained values from [19, 21,52-54]. The applicability to multi-exponential decay functions is more or less theoretical. Resolution of double exponential decay functions in FRET systems has been proved for TCSPC only.

The maximum count rate of the TCSPC method was defined as the rate at which the counting efficiency drops to 50%. Therefore, the values are smaller that the reciprocal dead time.

Technique		F Figure of Merit	E Effi-ciency	Reso-lution ps	Count Rate MHz	Multi-Epon. Decay	Fast Scan	Con-focal	Remark
Gated Image Intensifier	200ps	4	0.057	20	unlim.	yes	yes	no	applicable for wide field
Single Channel mod.	Sinewave	3.7	0.07	300	unlim.	yes	no	yes	slow scan only
Technique	Dirac	1.1	0.95	300	unlim.	yes	no	yes	
Modulated Image	Sinewave	10	0.01	300	unlim.	yes	yes	no	applicable for
Intensifier	Dirac	4.3	0.054	300	unlim.	yes	yes	no	wide field
Multi-Gate SPC	2 Gates	1.5-2.1	0.7-0.8	100	30	no	no	yes	
	8 Gates	1.1-1.5	0.8-0.95	<100	30	yes	no	yes	
2 λ Channels	2 Gates, 4 Detectors	0.78-1.06	0.97-1.13	100	120	no	no	yes	
TCSPC Imaging,	100 kHz [4]	1	1	2.5 [3]	4 [1]	yes	yes	yes	1 detector
1 TCSPC Channel	1 MHz [4]	1.06	0.88	2.5 [3]	4 [1]	yes	yes	yes	
TCSPC Imaging	100 kHz [4]	0.71 [5]	2 [5]	2.5 [3]	16 [2]	yes	yes	yes	4 detectors,
4 TCSPC Channels,	1 MHz [4]	0.72	1.94	2.5 [3]	16 [2]	yes	yes	yes	4 parallel TCSPC
4 λ Channels,	4 MHz [4]	0.75	1.76	2.5 [3]	16 [2]	yes	yes	yes	channels
2 Chromophores	10 MHz [4]	1.07	0.88						
TCSPC Multiwave-	100 kHz [4]	0.71 [5]	2 [5]	2.5 [3]	4 [1]	yes	yes	yes	up to 16 detector
length Imaging,	1 MHz [4]	0.75	1.76	2.5 [3]	4 [1]	yes	yes	yes	channels recording
2-16 λ Channels,									simultaeously in
2 Chromophores									1 TCSPC channel

1) Count rate for 50% counting loss. Dead time 150ns
2) Count rate for 50% counting loss. Four parallel channels with a dead time of 150ns each
3) With MCP-PMT
4) Overall count rate
5) F < 1 and E > 1 because 2 chromophores are detected simultaneously and the system is compared with a single channel detecting only 1 chromophore

Summary

A wide variety of lifetime imaging techniques for time-resolved microscopy is available - gated and modulated image intensifiers, single channel modulation techniques and gated and time-correlated single photon counting. At the same time two generally different microscopy techniques exist - the wide field microscope and the confocal or two-photon laser scanning microscope.

For wide field microscopy the gated and modulated image intensifiers and can be used. Wide-field lifetime systems do not have the intrinsic depth resolution and optical sectioning capability of the confocal and two-photon scanning systems.

For laser scanning microscopes the best results are achieved with multi-gate photon counting and with the TCSPC imaging technique. Multi-gate photon counting can be used up to very high count rates and efficiently detects single exponential lifetimes down to a few 100ps. It does, however, not reach the efficiency and the time-resolution of TCSPC. It is not clear how far the high count rate of the technique can be practically exploited because photobleaching sets a limit to the fluorescence intensity obtained from the excited sample volume.

TCSPC is able to detect lifetimes down to a few ps and is able to resolve the components of multi-exponential decay functions. It has a near-ideal efficiency and is able to detect in several wavelength intervals simultaneously. Moreover, the TCSPC technique can be used to obtain combined

FCS / lifetime data in selected spots of a sample. TCSPC imaging works at an extremely high scanning speed and is therefore compatible to almost any laser microscope.

Among all methods TCSPC imaging with confocal or two-photon microscopes scanning microscopes is most suitable to meet the requirements of cell imaging - optical sectioning, multi-wavelength recording, high detection efficiency, high time resolution, resolution of multi-exponential decay functions, and applicability of FCS techniques.

References

[1] M. Minsky : Memoir on inventing the confocal microscope. Scanning 10, 128-138 (1988).

[2] J.G. White, W.B. Amos, M. Fordham : An evaluation of confocal versus conventional imaging of biological structures by fluorescence light microscopy. J. Cell Biol. 105, 41-48 (1987).

[3] W. Denk, J.H. Strickler, W.W. Webb, Two-photon laser scanning fluorescence microscopy. Science 24 (1990) 73-76

[4] A. Periasami, M. Elangovan, H. Wallrabe, J.N. Demas, M. Barroso, D.L. Brautigan, R.N. Day, Methods in cellular imaging (ed. by A. Periasamy), 295-308, Oxford University Press, New York

[5] B. Herman, Fluorescence Microscopy, 2nd. edn. Springer-Verlag, New York 1998

[6] J.R. Lakowicz, Principles of Fluorescence Spectroscopy, 2nd. Ed., Plenum Press, New York 1999

[7] A. Periasami, R.N. Day, Visualizing protein interactions in living cells using digitized BFG imaging and FRET microscopy, in: Green Fluorescent Proteins, ed. by K.F. Sullivan, S.A Key, Academic Press, 1999

[8] M. Elangovan, R.N. Day, A. Periasami, Nanosecond fluorescence resonance energy transfer-fluorescence lifetime imaging microscopy to localize the protein interactions in a single cell. J. Microsc. 205 (2002) 3-14

[9] W.R.G. Baeyens, D. de Keukeleire, K. Korkidis, Luminescence techniques in chemical and biochemical analysis, M. Dekker, New York, 1991

[10] M.R. Eftink, Fluorescence quenching: Theory and application, in: J.R. Lakowicz, Topics in fluorescence spectrocopy, Vol. 2 (1991) 53-126

[11] M.A.M.J. van Zandvoort, W. Engels, C.J. de Grauw, H.C. Gerritsen, D.W. Slaaf, Lifetime imaging of the vital DNA/RNA probe SYTO13 in helthy and apoptitic cells. Proc. SPIE 4626-83 (2002)

[11a] Van Zandvoort, M.A.M.J., de Grauw, C.J., Gerritsen, H.C., Broers, J.L.V., Egbrink, M.G.A. Ramaekers, F.C.S., Slaaf, D.W. Discrimination of DNA and RNA in cells by a vital fluorescent probe: Lifetime imaging of SYTO13 in healthy and apoptotic cells. Cytometry 47 (2002) 226-223

[11b] Gerritsen, H.C., Sanders, R., Draaijer, A., Levine, Y.K. Fluorescence lifetime imaging of oxygen in cells. J. Fluoresc. **7** (1997) 11-16

[12] Jens-Peter Knemeyer, Nicole Marmé, Markus Sauer, Probes for detection of specific DNA sequences at the single molecule level. Anal. Chem. 72 (2000) 3717-3724

[13] M. E. Dickinson, C.W. Waters, G. Bearman, R. Wolleschensky, S. Tille, S.E. Fraser, Sensitive imaging of spectrally overlapping fluorochromes using the LSM 510 Meta. Proc. SPIE 4620 (2002)

[14] Thomson, N,L., Fluorescence Correlation Spectrocopy. Topics in Fluorescence Spectroscopy, Vol. 1, ed. by J.R. Lakowicz, 337-378. Plenum Press, New York, 1991

[15] K.M. Berland, P.T.C. So, E. Gratton, Two-photon fluorescence correlation spectroscopy: Method and application to the intracellular environment. Biophys. J. 88 (1995) 694-701

[16] P. Schwille, S. Kummer, A.H. Heikal, W.E. Moerner, W.W. Webb, Fluorescence correlation spectroscopy reveals fast optical excitation-driven intramolecular dynamics of yellow fluorescent proteins. PNAS 97 (2000) 151-156

[17] Michael Prummer, Christian Hübner, Beate Sick, Bert Hecht, Alois Renn, Urs P. Wild, Single-Molecule Identification by Spectrally and Time-Resolved Fluorescence Detection. Anal. Chem. 2000, 72, 433-447

[18] J. Schaffer, A. Volkmer, C. Eggeling, V. Subramaniam, C. A. M. Seidel, Identification of single molecules in aqueous solution by time-resolved anisotropy. Journal of Physical Chemistry A, 103 (1999) 331-335

[19] P.T.C. So, T. French, E. Gratton, A frequency domain microscope using a fast-scan CCD camera. Proc. SPIE 2137 (1994) 83-92

[20] M. Straub, S. W. Hell, Fluorescence lifetime three-dimensional microscopy with picosecond precision using a multifocal multiphoton mocroscope. Appl. Phys. Lett. 73 (1998) 1769-1771

[21] A. Squire, P.J. Verveer, P.I.H. Bastiaens: Multiple frequency fluorescence lifetime imaging microscopy. J. Microsc. 197, 136-149 (2000).

[22] M.A. Neil, A. Squire, R. Juskaitas, P.I. Bastiaens, T. Wilson, Wide-field fluorescence microscopy with laser illumination. J. Microsc. 197 (2000) 1-4

[23] M.J. Cole, J.Siegel, R. Dowling, M.J. Dayel, D. Parsons-Karavassilis, P.M. French, M.J. Lever, L.O. Sucharov, M.A. Neil, R. Juskaitas, T. Wilson, Time-domain whole-field lifetime imaging with optical sectioning. J. Microsc. 203 (2001) 246-257

[24] Betzig, E., Trautmann, J.K., Near-field optics: Microscopy, spectroscopy and surface modification beyond the diffraction limit. Science 257, 189-195

[25] Betzig, E., Trautmann, J.K.,Harris, T.D., Weiner, J.S., Kostelak, R.L., Breaking the diffraction barrier: Optical microscopy on a nanometric scale. Science 251 (1991) 1468-1470

[26] Dunn, R.C. Near-field scanning optical microscopy. Chem. Rev. 99 (1999) 2891-2928

[27] Hollars, C.W., Dunn, R.C., Submicron fluorescence, topology, and compliance measurements of phase-separated lipid monolayers using tapping-mode near-fiel scanning optical microscopy. J. Phys. Chem. B. 101, 6313-6317

[28] Kirsch, A.K., Subramaniam, V., Jenei, A., Jovin, T.M., Fluorescence Resonance transfer detected by scanning near-field optical microscopy. J. Microsc. 194 (1999) 448-454

[29] Femtolight series fiber lasers, IMRA America Inc., www.imra.com

[30] Pulsed diode lasers, PicoQuant GmbH, www.picoquant.com

[31] BDL-450 picosecond diode laser. www.becker-hickl.com

[32] BHL-250 pulsed diode lasers. www.becker-hickl.com

[33] M. Kress, Th. Meier, T. A. A. El-Tayeb, R. Kemkemer, R. Steiner, A. Rück, Short-pulsed diode lasers as an excitation source for time-resolved fluorescence applications and confocal laser scanning microscopy in PDT, Proc. SPIE 4431(2001)

[33a] A. Rück, F. Dolp, C. Happ, R. Steiner, M. Beil, Fluorescence lifetime imaging (FLIM) using ps pulsed diode lasers in laser scanning microscopy. Proc. SPIE 4962-44 (2003)

[34] Hidehiro Kume (Chief Editor), Photomultiplier Tube, Hamamatsu Photonics K.K., 1994

[35] SPCM-AQR series. www.perkinelmer.com/opto

[36] S. Cova, S. Lacaiti, M.Ghioni, G. Ripamonti, T.A. Louis, 20-ps timing resolution with single-photon avalanche photodiodes, Rev. Sci. Instrum. 60, 1989, 1104-1110

[37] M. Nagorni, S. W. Hell, 4Pi-confocal microscopy provides three-dimensional images of the microtubule network with 100- to 150-nm resolution. J. of Structural Biology 123 (1998) 236-247

[38] Ballew, R.M., Demas, J.N., An error analysis of the rapid lifeetime determination method for the evaluation of single exponential decays. Anal. Chem. 61 (1989) 30-33

[39] K. Carlsson, J.P. Philip, Theoretical Investigation of the Signal-to-Noise ratio for different fluorescence lifetime imaging techniques. Proc. SPIE 4622-08 (2002)

[40] J. Widengreen, R. Rigler, Mechanisms of photobleaching investigated by fluorescence correlation spectroscopy. Bioimaging 4 (1996) 149-157

[41] A.A. Heikal, W.W. Webb, One- and two-photon time-resolved fluorescence spectroscopy of selected fluorescent markers: photobleaching, triple-, and singlet-state dynamics. Biophys. J. 73 (1999) 260

[42 E.J. Sánchez, L. Novotny, G.R. Holtom, X.S. Xie. Room-Temperature fluorescence imaging and spectroscopy of single molecules by two-photon fluorescence. J. Phys. Chem. A 101 (1997) 7019-7023

[43] G.H. Patterson, D.W. Piston, Photobleaching in two-photon exciatation microscopy. Biophys. J. 78 (2000) 2159-2162

[44]G. J. Brakenhoff, M. Müller, R.I. Grauharali, Analysis of efficiency of two-photon versus single-photon absorption for fluorescence generation in biological objects. J. Microsc. 183 (1996) 140-144

[45] Hopf, A., Neher, E., Highly nonlinear Photodamage on two-photon fluorescence microscopy. Biophysical Journal 80 (1002) 2029-2036

[46] K. König, P.T.C. So, W.W. Mantulin, B.J. Tromberg, E. Gratton, Two-Photon excited lifetime imaging of autofluorescence in cells during UVA and NIR photostress. J. Microsc. 183, 197-204

[47] K. Koenig, T.W. Becker, P. Fischer, I. Riemann, K.-J. Halbhuber, Pulse-length dependence of cellular response to intense near-infrared pulses in multiphoton microscopes. Opt. Lett. 24 (1999) 113-115

[48] J. Bewesdorf, R. Pick, S. W. Hell, Multifocal multiphoton microscopy. Opt. Lett. 23 (1998) 655-657

[49] A.H. Buist, M. Müller, J. Squier, G.J. Brakenhoff, Real time two-photon absorption microscopy using multi-point excitation. Journal of Microscopy 192 (1998) 21767-226

[50] P. Urayama, J.A. Beamish, F.K. Minn, E.A. Hamon, M.-A. Mycek, A UV fluorescence lifetime imaging microscope to probe endogenous cellular fluorescence. CLEO 2002, Technical Digest, CTh062

[51] Pico Star Camera, www.lavision.com

[52] K. Carlsson, A. Liljeborg, Simultaneous confocal lifetime imaging of multiple fluorophores using the intensity-modulated multiple-wavelength scanning (IMS) technique. J. Microsc. 191 (1998) 119-127

[53] K. Carlsson, A. Liljeborg, Confocal fluorescence microscopy using spectral and lifetime information to simultaneaously record four fluorophores with high channel separation. J. Microsc. 185 (1997) 37-46

[54] P.T.C. So, T. French, W.M. Yu, K.M. Berland, C.Y. Dong, E. Gratton, Time-resolved fluorescence microscopy using two-photon excitation. Bioimaging 3 (1995) 49-63

[55] P.T.C. So, T. French, E. Gratton, A frequency domain microscope using a fast-scan CCD camera. Proc. SPIE 2137 (1994) 83-92

[56] A. Squire, P.J. Verveer, P.I.H. Bastiens: Multiple frequency fluorescence lifetime imaging microscopy. J. Microsc. 197, 136-149 (2000).

[57] E.P. Buurman, R. Sanders, A. Draaijer, H.C. Gerritsen, J.J.F. van Veen, P.M. Houpt, Y.K. Levine, Fluorescence lifetime imaging using a confocal laser scanning microscope. Scanning 14, 155-159 (1992).

[58] J. Sytsma, J.M. Vroom, C.J. de Grauw, H.C. Gerritsen, Time-gated fluorescence lifetime imaging and microvolume spectroscopy using two-photon excitation. Journal of Microscopy, 191 (1998) 39-51

[59] H7422 data sheet, Hamamatsu Photonics, www.hamamatsu.com

[60] R3809U data sheet, Hamamatsu Photonics, www.hamamatsu.com

[61] Scully, A.D., Ostler, R.B., Phillips, D., O'Neill, P.O., Townsend, K.M.S., Parker, A.W., McRobert, A.J., Application of fluorescence lifetime imaging microscopy to the investigation of intracellular PDT mechanisms. Bioimaging 5 (1997) 9-18

[62] D.V. O'Connor, D. Phillips, Time Correlated Single Photon Counting, Academic Press, London 1984

[63] SPC-134 through SPC-730 TCSPC Modules, Operating Manual and TCSPC Compendium. Becker & Hickl GmbH, www.becker-hickl.com

[64] W. Becker, H. Stiel, E. Klose, Flexible Instrument for time-correlated single photon counting, Rev. Sci. Instrum. 62 (1991) 2991-2996

[65] I. Bugiel, K. König, H. Wabnitz, Investigations of cells by fluorescence laser scanning microscopy with subnanosecond resolution. Lasers in the Life Sciences 3 (1989) 47-53

[66] W. Becker, A. Bergmann, H. Wabnitz, D. Grosenick, A. Liebert, High count rate multichannel TCSPC for optical tomography. Proc. SPIE 4431, 249-254 (2001)

[67] W. Becker, A. Bergmann, K. Koenig, U. Tirlapur, Picosecond fluorescence lifetime microscopy by TCSPC imaging. Proc. SPIE 4262 (2001) 414-419

[68] Wolfgang Becker, Klaus Benndorf, Axel Bergmann, Christoph Biskup, Karsten König, Uday Tirplapur, Thomas Zimmer, FRET Measurements by TCSPC Laser Scanning Microscopy, Proc. SPIE 4431(2001) 94-98

[69] Wolfgang Becker, Axel Bergmann, Georg Weiss, Lifetime Imaging with the Zeiss LSM-510. Proc. SPIE 4620 (2002) 30-35

[70] K. Koenig, C. Peuckert, I. Riemann, U. Wollina, Optical tomography of human skin with picosecond time resolution using intense near infrared femtosecond laser pulses, Proc. SPIE 4620-36

[71] S. Ameer-Beg, P.R. Barber, R. Locke, R.J. Hodgkiss, B. Vojnovic, G.M. Tozer, J. Wilson, Application of multiphoton steady state and lifetime imaging to mapping of tumor vascular architecture in vivo. Proc. SPIE 4620 (2002) 85-95

[72a] Wolfgang Becker, Axel Bergmann, Christoph Biskup, Thomas Zimmer, Nikolaj Klöcker, Klaus Benndorf, Multi-wavelength TCSPC lifetime imaging. Proc. SPIE 4620 (2002) 79-84

[72b] Wolfgang Becker, Axel Bergmann, Christoph Biskup, Laimonas Kelbauskas, Thomas Zimmer, Nikolaj Klöcker, Klaus Benndorf, High resolution TCSPC lifetime imaging. Proc. SPIE 4963-30 (2003)

[73] A. Schönle, M. Glatz, S. W. Hell, Four-dimensional multiphoton microscopy with time-correlated single photon counting. Appl. Optics 39 (2000) 6306-6311

[74] S. Jakobs, V. Subramaniam, A. Schönle, Th. Jovin, S.W. Hell, EGFP and DsRed expressing cultures of escherichia coli imaged by confocal, two-photon and fluorescence lifetime microscopy. FEBS Letters 479 (2000) 131-135

[75] D. Schweitzer, A. Kolb, M. Hammer, E. Thamm, Tau-mapping of the autofluorescence of the human ocular fundus. Proc. SPIE Vol. 4164, 79-89

[75b] D. Schweitzer, A. Kolb, M. Hammer, E. Thamm, Basic investigations for 2-dimensional time-resolved fluorescence measurements at the fundus. International Ophthalmology 23 (2001) 399-404

[76] HRT-41, HRT-81, HRT-82 Routing Devices, Operating Manual. Becker & Hickl GmbH, www.becker-hickl.com

[77] PML-16 16 Channel Detector Head, Operating Manual. Becker & Hickl GmbH, www.becker-hickl.com

[78] E-S. Kwak, T.J.Kang, A.A. Vanden Bout, Fluorescence lifetime imaging with near-field scanning optical microscopy. Anal. Chem. 73 (2001) 3257-3262

[79] W. Hartmann, F. Bernhard, Fotovervielfacher und ihre Anwendung in der Kernphysik. Akademie-Verlag Berlin 1957

[80] M. Köllner, J. Wolfrum, How many photons are necessary for fluorescence-lifetime measurements? Phys. Chem. Lett. 200 (1992) 199-204

[81] Gerritsen, H.C., Asselbergs, M.A.H., Agronskaia, A.V., van Sark, W.G.J.H.M., Fluorescence lifetime imaging in scanning microscopes: acquistition speed, photon economy and lifetime resolution. J. Microsc. 206 (2002) 218-224

[82] L. Kelbauskas, W. Dietel, Internalization of aggregated photosensitizers by tumor cells: Subcellular time-resolved fluorescence spectroscopy on derivates of pyropheophorbide-a ethers and chlorin e6 under femtosecond one- and two-photon excitation. Photochem. Photobiol. 76 (2002) 686-694